Rigidly Foldable 2D Tilings

THESIS

submitted in partial fulfillment of the
requirements for the degree of

BACHELOR OF SCIENCE
in
PHYSICS AND MATHEMATICS

Author :	N. Vasmel
Student ID :	1282131
Supervisor Physics:	Prof.dr. M. van Hecke
	Msc. P. Dieleman
Supervisor Mathematics :	Dr. F. Spieksma

Leiden, The Netherlands, July 20, 2016

Rigidly Foldable 2D Tilings

N. Vasmel

Huygens-Kamerlingh Onnes Laboratory, Leiden University
P.O. Box 9500, 2300 RA Leiden, The Netherlands

Mathematical Institute Leiden, Leiden University
P.O. Box 9512, 2300 RA Leiden, The Netherlands

July 20, 2016

Abstract

The proposed research is for research into the rigid folding of 2D tilings. We will show that the folding behaviour of a 4-vertex is very similar to that of its mirror image, and its supplement. We will show how we can use this to combinatorially design large rigidly foldable tilings. We will study in how many different ways these tilings can fold. Finally we will also discuss the mountain-valley patterns according to which these tilings will fold and give a method to design a tiling that folds according to a given mountain-valley pattern. We also discuss how we can apply restrictions on certain folds in a tiling to force it into a specific folded state.

Contents

Chapter 1

Introduction

In this thesis we study a system of rigid quadrilateral plates which are connected to each other by hinges at their sides. The corners of four of these quadrilaterals meet in points, which we will call 4-vertices. We only consider 4-vertices whose sum of angles is 2π. These systems we call *4-vertex origami patterns*.

These origami patterns are in general overconstrained. However, under additional requirements, patterns can be designed that have one degree of freedom and fold rigidly, meaning that the plates stay planar while the creases are allowed to deform, see examples in fig. 1.1. To achieve this usually periodic patterns with some small unit cell of quadrilateral plates are used [1–4]. In [5] a method was described to numerically find a rigidly foldable pattern if the sum of opposite angles in each vertex is π. We will develop a method based on combinatorics to design rigidly foldable tilings without the need of a unit cell or this requirement on the angles.

There are many applications to origami patterns. One of the best known examples of a rigidly foldable 4-vertex pattern is the Miura-ori pattern, which was developed for folding solar panels such that they could be transported more easily into outer space [2]. An other application is creating 3-dimensional structures from 2-dimensional sheets of material [6]. There also is an interest in origami for use in architectural design [7].

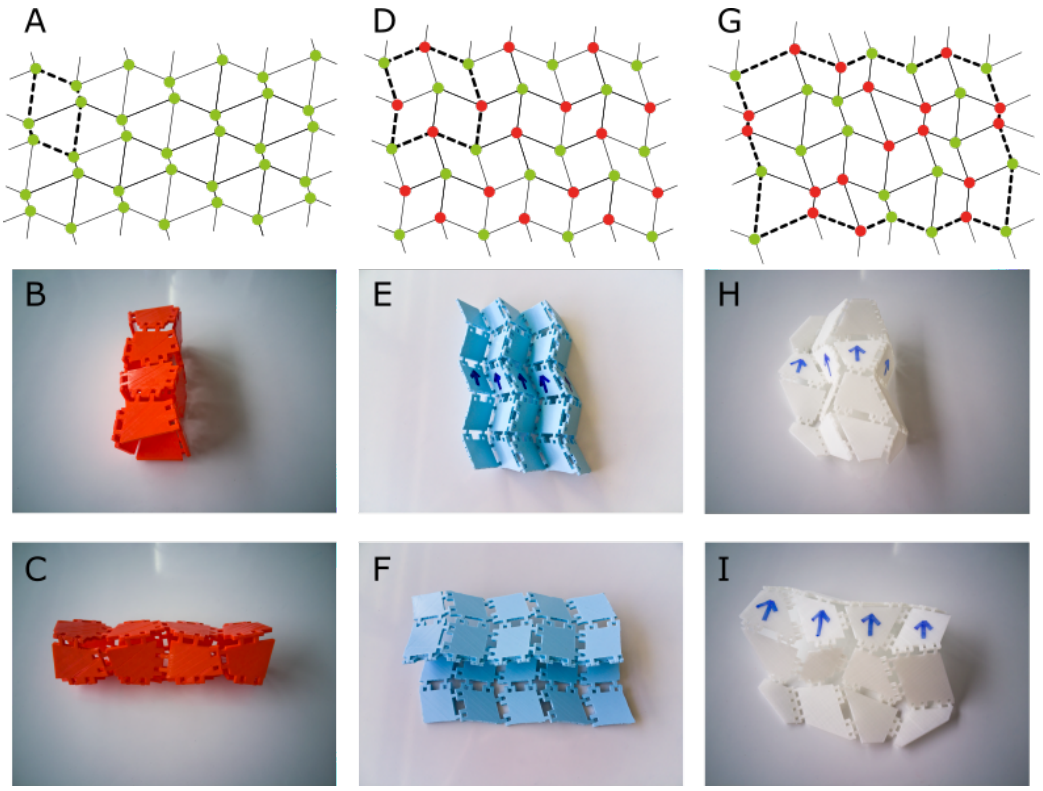

Figure 1.1: ***A****: The Hufmann-tesselation [1] existing of a single 4-vertex and its rotation placed on a grid.* ***B,C****: Two different folded states of* ***A****.* ***D****: The Mars-pattern [3], a pattern consisting of a vertex (green) and its supplemented mirror image (red) placed on a grid.* ***E,F****: Two different folded states of* ***D****.* ***G****: A newly created pattern consisting of a vertex (green) and its supplemented mirror image (red) placed on a grid.* ***H,I****: Two folded states of* ***G****.*

Outline

In chapter 2 we will describe the folding behaviour of a single vertex. We will also note the similarities in folding between a vertex, its mirror image, and its supplement. In chapter 3 we use this to create different rigidly foldable systems of 3×3 quadrilaterals. In chapter 4 we will combine several of these 3×3 systems to design much larger patterns. We will also have a look at the amount of different folded states we can achieve for the different patterns. In chapter 5 we will look at mountain-valley patterns, which describe the folded states. We will determine which mountain-valley patterns are possible and how to design tilings which will fold according to a given mountain-valley pattern.

In section 6.2 we will discuss the contribution this thesis makes in terms of new results.

Chapter 2

Single Generic 4-Vertex

2.1 General Information

A single 4-vertex can be represented by the sector angles a, b, c, d of 4 wedge-shaped plates that meet at a single point. The 4-vertex is called a *flat vertex* if the sector angles obey the relation $a + b + c + d = 2\pi$, fig. 2.1.

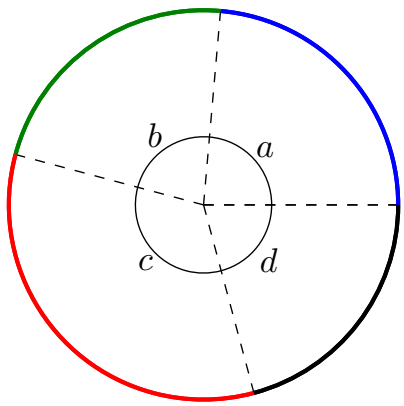

Figure 2.1: *A flat vertex with sector angles a, b, c and d.*

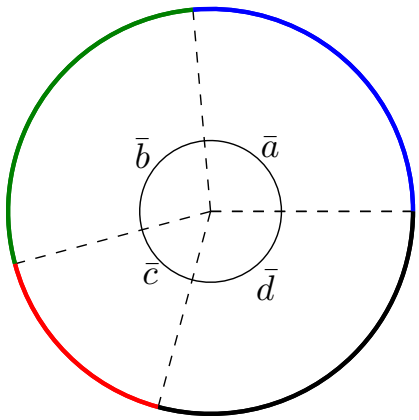

Figure 2.2: *The supplement of the vertex in fig. 2.1.*

We say that a vertex is *rigidly foldable* if it can be deformed such that the sector angles are constant while the dihedral angles between the plates change. See fig. 2.3 for an example of a folded vertex.

A 4-vertex is only rigidly foldable when all the sector angles are smaller than π and not both pairs of opposite sector angles are the same [8]. In the special case where the alternating sum of the sector angles is 0, the vertex

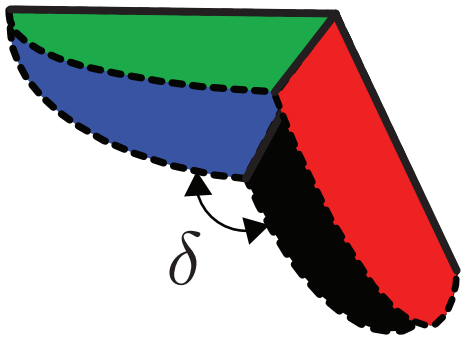

Figure 2.3: *A folded vertex. δ Is the dihedral angle between the blue and the black plate.*

is called *flat-foldable* (Kawasaki's theorem [9]). If a vertex is flat-foldable, there is a folded state where all the dihedral angles are 0 or 2π. Most research into mesh origami focuses on these types of vertices. Primarily, since the existence of a folded state of flat-foldable mesh origami with a dihedral angle $\delta \in (0, \pi) \cup (\pi, 2\pi)$ guarantees the existence of a rigid folding motion [5].

However, we wish to study the generally underexposed generic folding. To do this we make an assumption that the angles $a, b, c, d, \bar{a} = \pi - a, \bar{b} = \pi - b, \bar{c} = \pi - c, \bar{d} = \pi - d \in (0, \pi)$ are all 8 distinct. The vertex containing the 4 supplemented angles $\bar{a}, \bar{b}, \bar{c}, \bar{d}$ in the same order as the unsupplemented angles in the original vertex we call the *supplemented vertex*, fig. 2.2. We will show that the folding of this supplemented vertex is very similar to that of the original one in section 2.2. We will also see that the mirror image of a vertex folds in a very similar manner.

For reasons of symmetry we wish to have some alternate version of the dihedral angles which are 0 in the unfolded state. To this end we introduce *folding angles* ρ. If the dihedral angle between two plates is $\delta \in [0, 2\pi]$ then the corresponding folding angle is $\rho = \delta - \pi$. Thus, $\rho \in [-\pi, \pi]$ and the folding angle is $\rho = 0$ in the unfolded state. The line where two plates meet, we will refer to as the *fold*.

We name the folding angles between the plates $\rho_1, \rho_2, \rho_3, \rho_4$. That is,

with ρ_1 the folding angle between plates d and a, ρ_2 between plates a and b, ρ_3 between plates b and c, and ρ_4 between plates c and d. We also introduce a more schematic depiction of the single vertex, fig. 2.4, in which the value of the angles and the fact whether or not the vertex is supplemented is ignored, while the orientation (mirrored or not) is preserved.

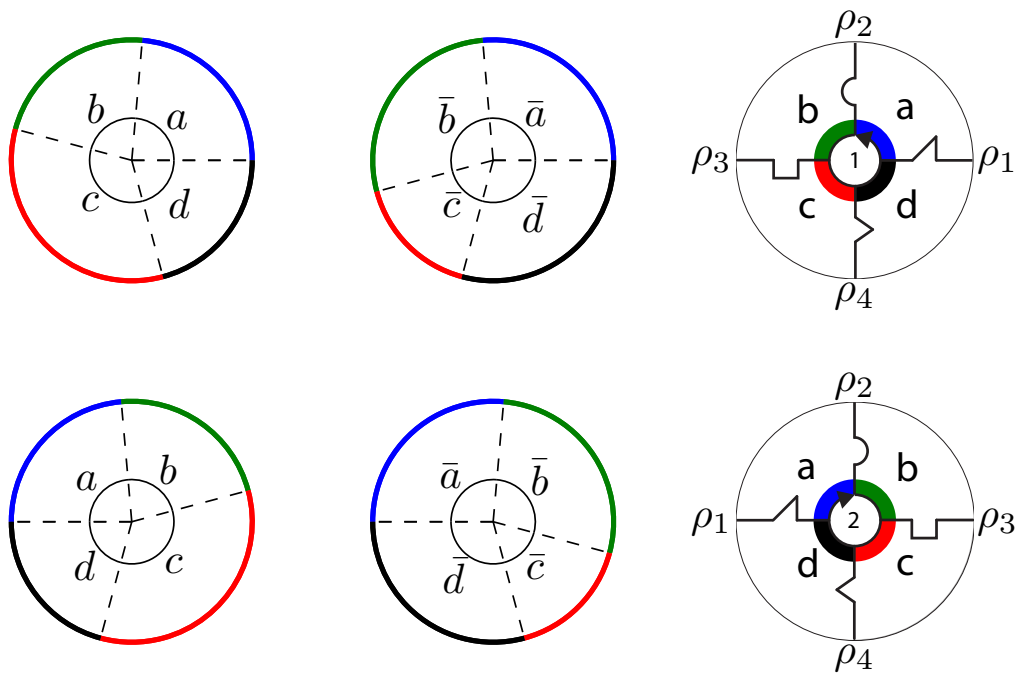

Figure 2.4: *A flat vertex with sector angles a, b, c and d is depicted at the top left. In the middle column its supplement is depicted and in the right column its schematic depiction. In the bottom row the same is done for the mirrored vertex.*

Folds with a positive folding angle are called *mountains* and folds with a negative folding angle are called *valleys*. Around a folded generic 4-vertex there are either three mountains and one valley or one mountain and three valleys [1, 8], we will refer to this as the *3-1 rule*. If a folding angle has its sign opposite to the signs of the other folding angles, it is called the *unique fold*.

Definition 2.1.1. For generic 4-vertices with 4 distinct angles $a, b, c, d \in (0, \pi)$ we call the plate corresponding to sector angle a the *unique plate* and the plate corresponding to sector angle c the *anti-unique plate* when

equations

$$d + a < b + c, \quad \text{and} \tag{2.1}$$
$$a + b < c + d \tag{2.2}$$

hold.

Note that we can always rename the sector angles such that sector angle a corresponds to the unique plate. Both folding angles enclosing the unique plate are capable of being the unique fold [10]. This gives rise to two distinct branches of folding motion for a single generic 4-vertex.

2.2 Folding Angle Relations

In order to find explicit expressions for the relations between the folding angles we use a new representation of a 4-vertex, a spherical 4-bar mechanism. We imagine placing a unit sphere around a single flat 4-vertex, and look at the projection of the 4-vertex on the spheres surface. The folds between adjoining plates are projected towards points on the spherical surface and these points are connected by arcs which are the projections of the sector angles (see fig. 2.5). The folding angles correspond to the angles between the arcs.

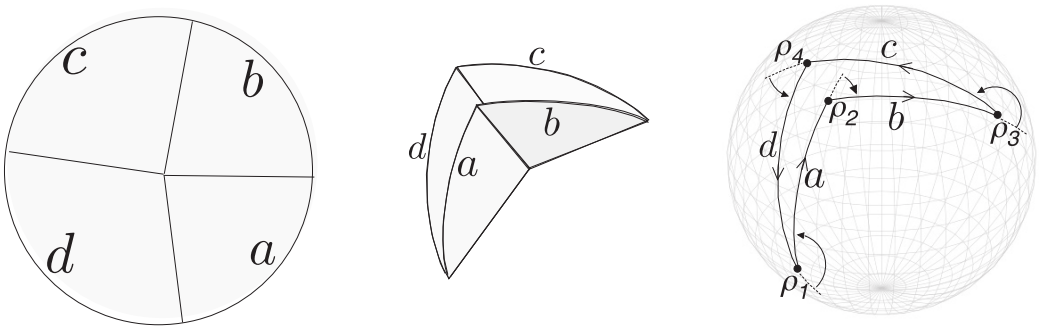

Figure 2.5: *An illustration of how a single flat 4-vertex can be folded and how it corresponds to a concave spherical quadrilateral. Figure from [10].*

We draw an additional arc connecting two opposite folds to transform the spherical quadrilateral into the sum (or difference) of two spherical triangles. With this, it is possible to use the spherical law of cosines and the spherical law of sines to express the folding angles as a function of each other and the sector angles.

As described in section 2.1, there are two unique folds and two distinct branches of motion for a generic 4-vertex, so we have to calculate the relations between the folding angles in two separate cases. The difference between the two unique folds will be acknowledged in this thesis by marking the different relations either as folding branch I or folding branch II. We rename the sector angles such that a corresponds to the unique plate.

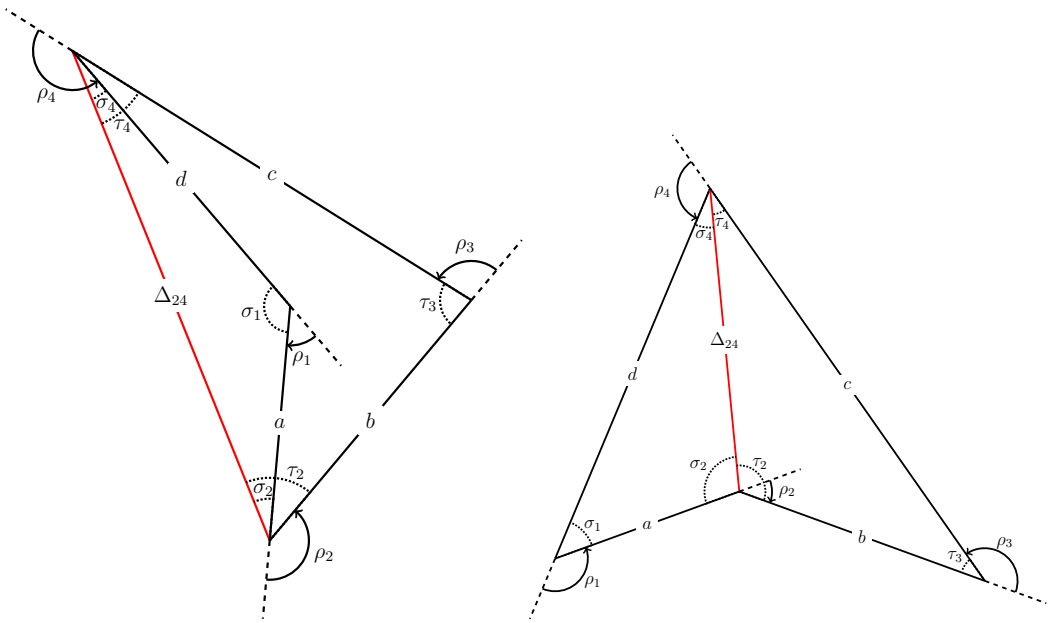

(a) *Branch I*
ρ_1 is the unique fold.

(b) *Branch II*
ρ_2 is the unique fold.

Figure 2.6: *A diagram showing how the spherical triangles on the spherical surface are created by drawing an arc connecting ρ_2 and ρ_4. The new angles created by these two spherical triangles are called $\sigma_1, \sigma_2, \sigma_4$ and τ_2, τ_3, τ_4 as depicted in the figure. For simplicity the triangles are depicted flat.*

From figures 2.6a and 2.6b we can deduce the relations between ρ_i, σ_i and τ_i. These equations hold for $\rho_3, \rho_4 \geq 0$; when $\rho_3, \rho_4 \leq 0$ one of the sides of the equations should be multiplied by -1. The superscript indicates which folding branch (I or II) is followed.

$$\begin{aligned}
\rho_1^I &= \sigma_1 - \pi & \rho_1^{II} &= \pi - \sigma_1 \\
\rho_2^I &= \pi + \sigma_2 - \tau_2 & \rho_2^{II} &= -\pi + \sigma_2 + \tau_2 \\
\rho_3^I &= \pi - \tau_3 & \rho_3^{II} &= \pi - \tau_3 \\
\rho_4^I &= \pi + \sigma_4 - \tau_4 & \rho_4^{II} &= \pi - \sigma_4 - \tau_4.
\end{aligned} \tag{2.3}$$

We now define a set of folding operators that map the folding angle of one fold onto that of any of the other folds, $\hat{\boldsymbol{\rho}}_{ij}\rho_j = \rho_i$, using spherical trigonometry and the identity $\arccos(-x) = \pi - \arccos(x)$.

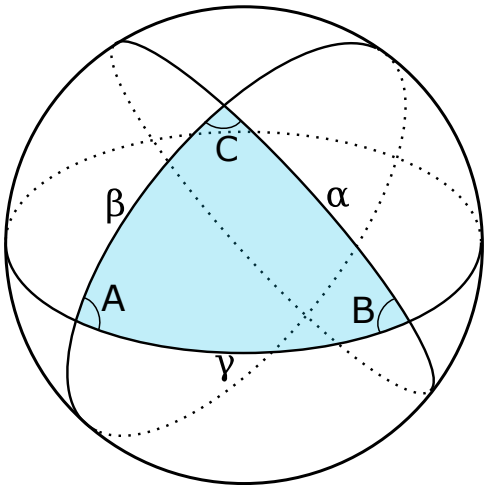

Figure 2.7: *A spherical triangle with sides of length α, β, γ and opposite angles A, B, C respectively.*

Theorem 2.2.1 (Spherical law of cosines and sines [11].)**.** *For a spherical triangle on a unit sphere, cf. fig. 2.7, with sides of length α, β, γ and opposite angles A, B, C respectively the following identities hold:*

$$\cos(\alpha) = \cos(\beta)\cos(\gamma) + \sin(\beta)\sin(\gamma)\cos(A), \text{ and} \tag{2.4}$$

$$\frac{\sin(A)}{\sin(\alpha)} = \frac{\sin(B)}{\sin(\beta)} = \frac{\sin(C)}{\sin(\gamma)}. \tag{2.5}$$

In the case of ρ_1 being the unique fold, denoted by folding branch I, we

use the above information to find the following set of equations:

$$\hat{\boldsymbol{\rho}}^{I}_{\mathbf{11}}\rho_1 = \rho_1, \tag{2.6}$$

$$\begin{aligned}\hat{\boldsymbol{\rho}}^{I}_{\mathbf{21}}\rho_1 = -\pi + \arccos\left(\frac{\cos\Delta_{24}\cos a - \cos d}{\sin a \sin\Delta_{24}}\right) \\ - \arccos\left(\frac{\cos\Delta_{24}\cos b - \cos c}{\sin b \sin\Delta_{24}}\right),\end{aligned} \tag{2.7}$$

$$\hat{\boldsymbol{\rho}}^{I}_{\mathbf{31}}\rho_1 = -\arccos\left(\frac{\cos b\cos c - \cos\Delta_{24}}{\sin b \sin c}\right), \tag{2.8}$$

$$\begin{aligned}\hat{\boldsymbol{\rho}}^{I}_{\mathbf{41}}\rho_1 = -\pi + \arccos\left(\frac{\cos\Delta_{24}\cos d - \cos a}{\sin d \sin\Delta_{24}}\right) \\ - \arccos\left(\frac{\cos\Delta_{24}\cos c - \cos b}{\sin c \sin\Delta_{24}}\right),\end{aligned} \tag{2.9}$$

where $\cos\Delta_{24} = \cos a\cos d - \sin a \sin d \cos\rho_1$. Δ_{24} is the shortest arc on the spherical surface between the points corresponding to folds ρ_2 and ρ_4, see figs. 2.6a, 2.6b.

In the case of ρ_2 being the unique fold, denoted by folding branch II, the following equations hold:

$$\hat{\boldsymbol{\rho}}^{II}_{\mathbf{11}}\rho_1 = \rho_1 \tag{2.10}$$

$$\begin{aligned}\hat{\boldsymbol{\rho}}^{II}_{\mathbf{21}}\rho_1 = -\pi + \arccos\left(\frac{\cos\Delta_{24}\cos a - \cos d}{\sin a \sin\Delta_{24}}\right) \\ + \arccos\left(\frac{\cos\Delta_{24}\cos b - \cos c}{\sin b \sin\Delta_{24}}\right),\end{aligned} \tag{2.11}$$

$$\hat{\boldsymbol{\rho}}^{II}_{\mathbf{31}}\rho_1 = \arccos\left(\frac{\cos b\cos c - \cos\Delta_{24}}{\sin b \sin c}\right), \tag{2.12}$$

$$\begin{aligned}\hat{\boldsymbol{\rho}}^{II}_{\mathbf{41}}\rho_1 = -\pi + \arccos\left(\frac{\cos\Delta_{24}\cos d - \cos a}{\sin d \sin\Delta_{24}}\right) \\ + \arccos\left(\frac{\cos\Delta_{24}\cos c - \cos b}{\sin c \sin\Delta_{24}}\right).\end{aligned} \tag{2.13}$$

We can find similar equations for the other folding operators. We use respectively

$$\begin{aligned}\cos\Delta_{13} &= \cos a\cos b - \sin a \sin b \cos\rho_2, \\ \cos\Delta_{24} &= \cos b\cos c - \sin b \sin c \cos\rho_3, \text{ and} \\ \cos\Delta_{13} &= \cos c\cos d - \sin c \sin d \cos\rho_4.\end{aligned}$$

$$\hat{\boldsymbol{\rho}}^{I}_{\mathbf{12}}\rho_2 = -\pi + \arccos\left(\frac{\cos\Delta_{13}\cos a - \cos b}{\sin a \sin\Delta_{13}}\right) + \arccos\left(\frac{\cos\Delta_{13}\cos d - \cos c}{\sin d \sin\Delta_{13}}\right), \tag{2.14}$$

$$\hat{\boldsymbol{\rho}}^{I}_{\mathbf{22}}\rho_2 = \rho_2, \tag{2.15}$$

$$\hat{\boldsymbol{\rho}}^{I}_{\mathbf{32}}\rho_2 = -\pi + \arccos\left(\frac{\cos\Delta_{13}\cos c - \cos d}{\sin c \sin\Delta_{13}}\right) + \arccos\left(\frac{\cos\Delta_{13}\cos b - \cos a}{\sin b \sin\Delta_{13}}\right), \tag{2.16}$$

$$\hat{\boldsymbol{\rho}}^{I}_{\mathbf{42}}\rho_2 = \arccos\left(\frac{\cos c \cos d - \Delta_{13}}{\sin c \sin d}\right). \tag{2.17}$$

$$\hat{\boldsymbol{\rho}}^{II}_{\mathbf{12}}\rho_2 = -\pi + \arccos\left(\frac{\cos\Delta_{13}\cos a - \cos b}{\sin a \sin\Delta_{13}}\right) - \arccos\left(\frac{\cos\Delta_{13}\cos d - \cos c}{\sin d \sin\Delta_{13}}\right), \tag{2.18}$$

$$\hat{\boldsymbol{\rho}}^{II}_{\mathbf{22}}\rho_2 = \rho_2, \tag{2.19}$$

$$\hat{\boldsymbol{\rho}}^{II}_{\mathbf{32}}\rho_2 = -\pi + \arccos\left(\frac{\cos\Delta_{13}\cos c - \cos d}{\sin c \sin\Delta_{13}}\right) - \arccos\left(\frac{\cos\Delta_{13}\cos b - \cos a}{\sin b \sin\Delta_{13}}\right), \tag{2.20}$$

$$\hat{\boldsymbol{\rho}}^{II}_{\mathbf{42}}\rho_2 = -\arccos\left(\frac{\cos c \cos d - \Delta_{13}}{\sin c \sin d}\right). \tag{2.21}$$

$$\hat{\boldsymbol{\rho}}^{I}_{\mathbf{13}}\rho_3 = -\arccos\left(\frac{\cos a \cos d - \cos\Delta_{24}}{\sin a \sin d}\right), \tag{2.22}$$

$$\hat{\boldsymbol{\rho}}^{I}_{\mathbf{23}}\rho_3 = \pi - \arccos\left(\frac{\cos\Delta_{24}\cos a - \cos d}{\sin a \sin\Delta_{24}}\right) + \arccos\left(\frac{\cos\Delta_{24}\cos b - \cos c}{\sin b \sin\Delta_{24}}\right), \tag{2.23}$$

$$\hat{\boldsymbol{\rho}}^{I}_{\mathbf{33}}\rho_3 = \rho_3, \tag{2.24}$$

$$\hat{\boldsymbol{\rho}}^{I}_{\mathbf{43}}\rho_3 = \pi - \arccos\left(\frac{\cos\Delta_{24}\cos d - \cos a}{\sin d \sin\Delta_{24}}\right) + \arccos\left(\frac{\cos\Delta_{24}\cos c - \cos b}{\sin c \sin\Delta_{24}}\right). \tag{2.25}$$

$$\hat{\boldsymbol{\rho}}^{\boldsymbol{II}}_{\mathbf{13}}\rho_3 = \arccos\left(\frac{\cos a \cos d - \cos \Delta_{24}}{\sin a \sin d}\right), \tag{2.26}$$

$$\begin{aligned}\hat{\boldsymbol{\rho}}^{\boldsymbol{II}}_{\mathbf{23}}\rho_3 = -\pi + \arccos\left(\frac{\cos \Delta_{24} \cos a - \cos d}{\sin a \sin \Delta_{24}}\right) \\ + \arccos\left(\frac{\cos \Delta_{24} \cos b - \cos c}{\sin b \sin \Delta_{24}}\right),\end{aligned} \tag{2.27}$$

$$\hat{\boldsymbol{\rho}}^{\boldsymbol{II}}_{\mathbf{33}}\rho_3 = \rho_3, \tag{2.28}$$

$$\begin{aligned}\hat{\boldsymbol{\rho}}^{\boldsymbol{II}}_{\mathbf{43}}\rho_3 = -\pi + \arccos\left(\frac{\cos \Delta_{24} \cos d - \cos a}{\sin d \sin \Delta_{24}}\right) \\ + \arccos\left(\frac{\cos \Delta_{24} \cos c - \cos b}{\sin c \sin \Delta_{24}}\right).\end{aligned} \tag{2.29}$$

$$\begin{aligned}\hat{\boldsymbol{\rho}}^{\boldsymbol{I}}_{\mathbf{14}}\rho_4 = -\pi + \arccos\left(\frac{\cos \Delta_{13} \cos a - \cos b}{\sin a \sin \Delta_{13}}\right) \\ + \arccos\left(\frac{\cos \Delta_{13} \cos d - \cos c}{\sin d \sin \Delta_{13}}\right),\end{aligned} \tag{2.30}$$

$$\hat{\boldsymbol{\rho}}^{\boldsymbol{I}}_{\mathbf{24}}\rho_4 = \arccos\left(\frac{\cos a \cos b - \Delta_{13}}{\sin a \sin b}\right), \tag{2.31}$$

$$\begin{aligned}\hat{\boldsymbol{\rho}}^{\boldsymbol{I}}_{\mathbf{34}}\rho_4 = -\pi + \arccos\left(\frac{\cos \Delta_{13} \cos c - \cos d}{\sin c \sin \Delta_{13}}\right) \\ + \arccos\left(\frac{\cos \Delta_{13} \cos b - \cos a}{\sin b \sin \Delta_{13}}\right),\end{aligned} \tag{2.32}$$

$$\hat{\boldsymbol{\rho}}^{\boldsymbol{I}}_{\mathbf{44}}\rho_4 = \rho_4. \tag{2.33}$$

$$\begin{aligned}\hat{\boldsymbol{\rho}}^{\boldsymbol{II}}_{\mathbf{14}}\rho_4 = \pi - \arccos\left(\frac{\cos \Delta_{13} \cos a - \cos b}{\sin a \sin \Delta_{13}}\right) \\ + \arccos\left(\frac{\cos \Delta_{13} \cos d - \cos c}{\sin d \sin \Delta_{13}}\right),\end{aligned} \tag{2.34}$$

$$\hat{\boldsymbol{\rho}}^{\boldsymbol{II}}_{\mathbf{24}}\rho_4 = -\arccos\left(\frac{\cos a \cos b - \Delta_{13}}{\sin a \sin b}\right), \tag{2.35}$$

$$\begin{aligned}\hat{\boldsymbol{\rho}}^{\boldsymbol{II}}_{\mathbf{34}}\rho_4 = \pi - \arccos\left(\frac{\cos \Delta_{13} \cos c - \cos d}{\sin c \sin \Delta_{13}}\right) \\ + \arccos\left(\frac{\cos \Delta_{13} \cos b - \cos a}{\sin b \sin \Delta_{13}}\right),\end{aligned} \tag{2.36}$$

$$\hat{\boldsymbol{\rho}}^{\boldsymbol{II}}_{\mathbf{44}}\rho_4 = \rho_4. \tag{2.37}$$

Note that the folding operators for the supplement sector angles $\bar{a} = \pi - a, \bar{b}, \bar{c}, \bar{d}$, as compared to the folding operators for the original sector angles a, b, c, d, are anti-symmetric when the sector angles are adjacent to one another (e.g. the folding operator $\hat{\boldsymbol{\rho}}^{\boldsymbol{I}}_{\mathbf{12}}$ becomes minus its original value), and exactly the same when the sectors are opposite to each other (e.g. the folding operator $\hat{\boldsymbol{\rho}}^{\boldsymbol{I}}_{\mathbf{13}}$ stays the same).

This follows from the expressions derived for the folding operators, but it can also be understood on a more intuitive level. We look at the last image of fig. 2.5 and imagine placing the antipodes ρ_1 and ρ'_3 of the points, where ρ_1 and ρ_3 are located, onto it. Next we trace the spherical quadrilateral from ρ'_1 to the point where ρ_2 is located to ρ'_3 to the point where ρ_4 is located and back to ρ'_1 on the surface of the sphere. Now we see that all the arc lengths become their own supplement and the folding angles ρ_1 and ρ_3 change sign, while ρ_2 and ρ_4 stay the same.

We introduce a schematic depiction of the operators by associating them to the corners of the depictions of the single vertex and its mirror image, fig. 2.1. We say that each sector of the vertex corresponds to the folding operator which maps the folds enclosing it onto each other going anti-clockwise. Thus, for a folding operator $\hat{\boldsymbol{\rho}}_{ij}$ the sector angle inside the tile corresponds to the sector angle of the single vertex enclosed by folds ρ_i and ρ_j. If (mod4) $j = i - 1$ then the vertex is oriented anti-clockwise (standard) and if $j = i + 1$ then the vertex is oriented clockwise (mirrored), fig. 2.8.

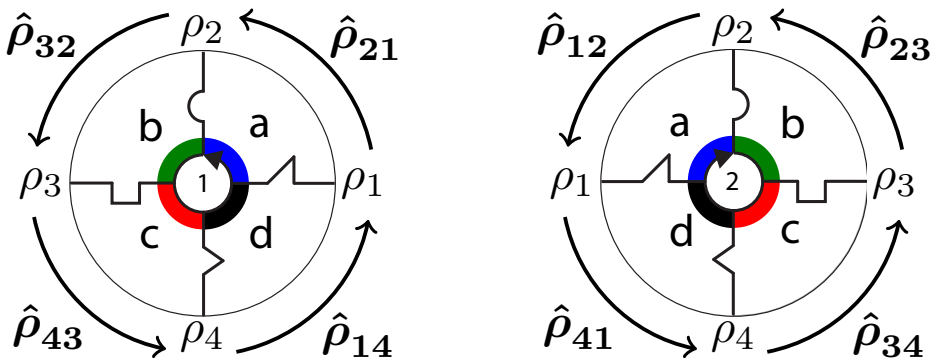

Figure 2.8: *A depiction of how we associate the folding operators to the corners in a vertex.*

Chapter 3

Rigidly Foldable Quadrilaterals

3.1 Kokotsakis Quadrilaterals

Definition 3.1.1. A *Kokotsakis quadrilateral* is a quadrilateral surface in $\mathbb{R}^3$ with 8 surrounding quadrilaterals, such that each internal vertex is a 4-vertex, fig. 3.1.

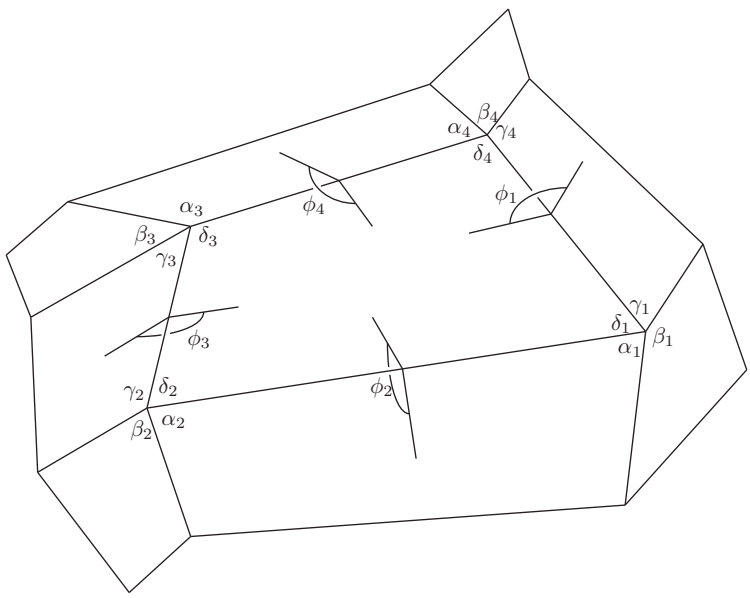

Figure 3.1: *A Kokotsakis quadrilateral. We named the angles of the inner vertices and the folding angles around the inner quadrilateral for reference in this section.*

In section 2.2 we derived equations for the folding angles around a single vertex. Composing these equations we can do the same for $\phi_1, \phi_2, \phi_3, \phi_4$, the folding angles around the sides of Kokotsakis quadrilateral.

Definition 3.1.2. A Kokotsakis quadrilatreal is *rigidly foldable* if there exists a non-constant one-paramater solution

$$(\phi_1(t), \phi_2(t), \phi_3(t), \phi_4(t)) \tag{3.1}$$

for the folding angles with the side lengths and sector angles fixed.

In general a Kokotsakis quadrilateral is over-constrained and not rigidly foldable [12]. A classification of all rigidly foldable Kokotsakis quadrilaterals was made in [13] by Izmestiev. We will list here the equations that are given by Izmestiev for the angles in fig. 3.1 for only those types with all $\phi_i(t)$ non-constant and flat vertices, i.e. the sum of angles of each vertex is 2π. We introduce the constants $\sigma_i = \beta_i + \delta_i - \alpha_i - \gamma_i$.

Isogonal type
In this type all vertices are flat-foldable. This means that

$$\alpha_i + \gamma_i = \beta_i + \delta_i = \pi, \qquad i \in \{1, 2, 3, 4\}. \tag{3.2}$$

Furthermore, for each vertex we introduce a constant κ_i, $i \in \{1, 2, 3, 4\}$, which can take two values corresponding to the two different folding branches

$$\kappa_i \in \left\{ \frac{\sin\frac{\alpha_i-\beta_i}{2}}{\sin\frac{\alpha_i+\beta_i}{2}}, \frac{\cos\frac{\alpha_i-\beta_i}{2}}{\cos\frac{\alpha_i+\beta_i}{2}} \right\}. \tag{3.3}$$

Now the quadrilateral is rigidly foldable iff for some choice of the κ_i

$$\kappa_1\kappa_3 = \kappa_2\kappa_4 \tag{3.4}$$

holds.

Linear compound type
In this case there is a linear relation between the half-tangents of the folding angles of a pair of opposite sides of the quadrilateral. We give the equations for all sector angles if $\tan\frac{\phi_1(t)}{2} = c\tan\frac{\phi_3(t)}{2}$. Similar equations can be found if $\tan\frac{\phi_2(t)}{2} = c\tan\frac{\phi_4(t)}{2}$. We have

$$\begin{aligned} \frac{\sin\alpha_1}{\sin\beta_1} &= \frac{\sin\alpha_2}{\sin\beta_2}, & \frac{\sin\gamma_1}{\sin\delta_1} &= \frac{\sin\gamma_2}{\sin\delta_2}, \\ \frac{\sin\alpha_3}{\sin\beta_3} &= \frac{\sin\alpha_4}{\sin\beta_4}, & \frac{\sin\gamma_3}{\sin\delta_3} &= \frac{\sin\gamma_4}{\sin\delta_4}, \end{aligned} \tag{3.5}$$

$$c = \pm\sqrt{\frac{\frac{\sin\gamma_2\sin\delta_2}{\sin\alpha_2\sin\beta_2}-1}{\frac{\sin\gamma_1\sin\delta_1}{\sin\alpha_1\sin\beta_1}-1}} = \pm\sqrt{\frac{\frac{\sin\gamma_4\sin\delta_4}{\sin\alpha_4\sin\beta_4}-1}{\frac{\sin\gamma_3\sin\delta_3}{\sin\alpha_3\sin\beta_3}-1}}, \tag{3.6}$$

where c is positive if σ_1 and σ_2 have the same sign and c is negative if they have the opposite sign. σ_1 And σ_2 have the same sign if and only if σ_3 and σ_4 have the same sign.

Equimodular type

$$\begin{aligned} \frac{\sin\alpha_1\sin\delta_1}{\sin\beta_1\sin\gamma_1} &= \frac{\sin\alpha_2\sin\delta_2}{\sin\beta_2\sin\gamma_2} & \frac{\sin\alpha_1\sin\beta_1}{\sin\gamma_1\sin\delta_1} &= \frac{\sin\alpha_2\sin\beta_2}{\sin\gamma_2\sin\delta_2} \\ \frac{\sin\alpha_3\sin\delta_3}{\sin\beta_3\sin\gamma_3} &= \frac{\sin\alpha_4\sin\delta_4}{\sin\beta_4\sin\gamma_4} & \frac{\sin\alpha_3\sin\beta_3}{\sin\gamma_3\sin\delta_3} &= \frac{\sin\alpha_4\sin\beta_4}{\sin\gamma_4\sin\delta_4} \end{aligned} \tag{3.7}$$

The so-called shift $t_i \in \mathbb{C}$ at each vertex is given by

$$\tan(t_i) = i\sqrt{\frac{\sin\beta_i\sin\delta_i}{\sin\alpha_i\sin\gamma_i}}. \tag{3.8}$$

The indeterminacy of the sifts is solved in the following table. Now the

	$p_iq_i \in \mathbb{R}_{>0}$	$p_iq_i \in i\mathbb{R}_{>0}$	$p_iq_i \in \mathbb{R}_{<0}$
$\sigma_i < 0$	$t_i \in i\mathbb{R}_{>0}$	$t_i \in \frac{\pi}{2} + i\mathbb{R}_{>0}$	$t_i \in \pi + i\mathbb{R}_{>0}$
$\sigma_i > 0$	$t_i \in \pi + i\mathbb{R}_{>0}$	$t_i \in \frac{3\pi}{2} + i\mathbb{R}_{>0}$	$t_i \in i\mathbb{R}_{>0}$

Table 3.1: *A table solving the indeterminacy of the shifts. Here we use the following equations* $p_i = \sqrt{\frac{\sin\alpha_i\sin\delta_i}{\sin\beta_i\sin\gamma_i}-1}$ *and* $q_i = \sqrt{\frac{\sin\gamma_i\sin\delta_i}{\sin\alpha_i\sin\beta_i}-1}$.

quadrilateral is rigidly foldable if there is a combination of pluses and minuses such that

$$\pm t_1 \pm t_2 \pm t_3 \pm t_4 \in 2\pi\mathbb{Z} \tag{3.9}$$

However, we are not just interested in all rigidly foldable Kokotsakis quadrilaterals, but specifically in those that can be folded in several different ways, each with one degree of freedom similarly to the single vertex. This is, because our objective is to be able to design a much larger system of connected quadrilaterals with multiple different folded states.

Another motivation for looking for a more specific kind of Kokotsakis quadrilaterals is, that when we link two rigidly foldable Kokotsakis quadrilaterals together, there is no guarantee they will still fold rigidly.

We call these larger systems of quadrilaterals connected in 4-vertices *4-vertex origami patterns*.

Theorem 3.1.1. *[12] A 4-vertex origami pattern with quadrilateral faces is rigidly foldable if and only if there is a choice of assigning folding branches to all vertices such that each Kokotsakis quadrilateral will rigidly fold accordingly.*

3.2 Tiles

In this section we will construct a specific set of rigidly foldable Kokotsakis quadrilaterals.. Each Kokotsakis quadrilateral in this set consists of a single generic 4-vertex (section 2.1) and its supplemented vertex and rotations placed around the inner vertices. We also call them the same if they have the same vertices after rotation of the quadrilateral, fig. 3.2. For these quadrilaterals we now introduce the concept of *tiles*. We call two Kokotsakis quadrilaterals the same tile if each of their inner vertices are the same or each others supplement. We will use the expressions we found for folding operators in section 2.2 to find which of these tiles are indeed rigidly foldable.

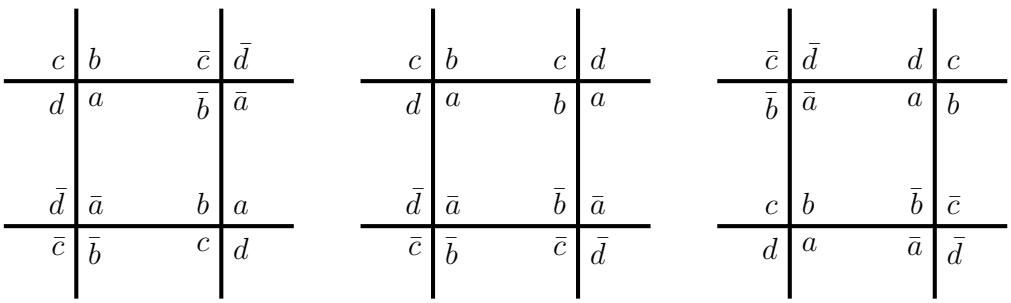

Figure 3.2: *On the left the inner angles of a schematic Kokotsakis quadrilateral are given. In the middle, two of the vertices are supplemented differently, but we will still regard these Kokotsakis quadrilaterals as the same tile. On the right a rotated version is given of the left Kokotsakis quadrilateral.*

We know that any composition of operators at a single vertex which maps a folding angle to itself, trivially has to be the identity operator. Using the equations found in section 2.2, we can also explicitly check that

they satisfy this condition, in other words:

$$\hat{\rho}_{12}\hat{\rho}_{23}\hat{\rho}_{34}\hat{\rho}_{41} = I, \tag{3.10}$$
$$\hat{\rho}_{14}\hat{\rho}_{43}\hat{\rho}_{32}\hat{\rho}_{21} = I, \text{ and} \tag{3.11}$$
$$\hat{\rho}_{ij}\hat{\rho}_{ji} = \hat{\rho}_{ji}\hat{\rho}_{ij} = I. \tag{3.12}$$

Precisely the same holds true for the composition of folding operators around the four different vertices of a rigidly foldable tile. So in order, to find the set of tiles we are looking for, we have to combine four of the folding operators such that they form the identity operator. Eqs. 3.10 and 3.11 are already in this form. We can combine two equations of the form of eq. 3.12 to find 32 other non-cyclic (since the tiles are allowed to rotate) permutations of four folding operators commuting to identity:

$$\hat{\rho}_{i+1,i}\hat{\rho}_{i,i+1}\hat{\rho}_{i+1,i}\hat{\rho}_{i,i+1} = I, \tag{3.13}$$
$$\hat{\rho}_{i,i+1}\hat{\rho}_{i+1,i}\hat{\rho}_{i+1,i}\hat{\rho}_{i,i+1} = I, \tag{3.14}$$
$$\hat{\rho}_{i+1,i}\hat{\rho}_{i,i+1}\hat{\rho}_{i+2,i-1}\hat{\rho}_{i-1,i+2} = I, \tag{3.15}$$
$$\hat{\rho}_{i+1,i}\hat{\rho}_{i,i+1}\hat{\rho}_{i+1,i+2}\hat{\rho}_{i+2,i+1} = I, \tag{3.16}$$
$$\hat{\rho}_{i,i+1}\hat{\rho}_{i+1,i}\hat{\rho}_{i+2,i+1}\hat{\rho}_{i+1,i+2} = I, \tag{3.17}$$
$$\hat{\rho}_{i+1,i}\hat{\rho}_{i,i+1}\hat{\rho}_{i+2,i+1}\hat{\rho}_{i+1,i+2} = I, \tag{3.18}$$
$$\hat{\rho}_{i+1,i}\hat{\rho}_{i,i+1}\hat{\rho}_{i-1,i+2}\hat{\rho}_{i+2,i-1} = I, \tag{3.19}$$
$$\hat{\rho}_{i,i+1}\hat{\rho}_{i+1,i}\hat{\rho}_{i+1,i+2}\hat{\rho}_{i+2,i+1} = I, \tag{3.20}$$
$$\hat{\rho}_{i,i+1}\hat{\rho}_{i+1,i}\hat{\rho}_{i+2,i-1}\hat{\rho}_{i-1,i+2} = I, \tag{3.21}$$

where $i = 1, 2, 3, 4$ and all subscripts are modulo 4. We call equations 3.10, 3.11, 3.13–3.21 the *loop conditions*. We remark that since the folding operator $\hat{\rho}_{ij}$ becomes $-\hat{\rho}_{ij}$ when the vertices are supplemented, there is an even number of supplemented vertices in each tile.

We can uniquely associate these loop conditions with tiles by associating a single folding operator with a sector angle and a (anti-)clockwise orientation of the single vertex, see fig. 2.8. For a folding operator $\hat{\rho}_{ij}$ the sector angle inside the tile corresponds to the sector angle of the single vertex enclosed by folds ρ_i and ρ_j. If (mod4) $j = i + 1$ then the vertex is oriented clockwise and if $j = i - 1$ then the vertex is oriented anti-clockwise. In fig. 3.5 all tiles corresponding to the loop conditions are given and in

fig. 3.3 a specific example is given. These schematic depictions are chosen such that two tiles fit together as puzzle pieces iff they have the same vertices (orientation and rotation) on the shared side. Since we only consider origami patterns of a single generic 4-vertex, its supplement, and its mirror image, we only need eight different corners to build up the entire tiling.

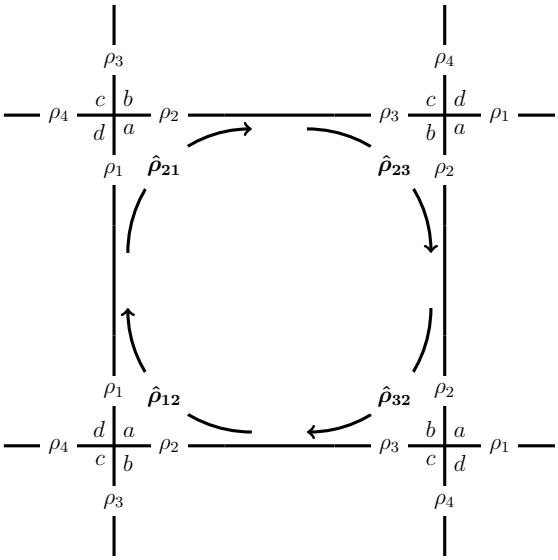

Figure 3.3: *Example of how we associate four folding operators with tiles. This tile corresponds to the combination of operators* $\hat{\rho}_{21}\hat{\rho}_{12}\hat{\rho}_{32}\hat{\rho}_{23}$*, eq. 3.18 with* $i = 1$.

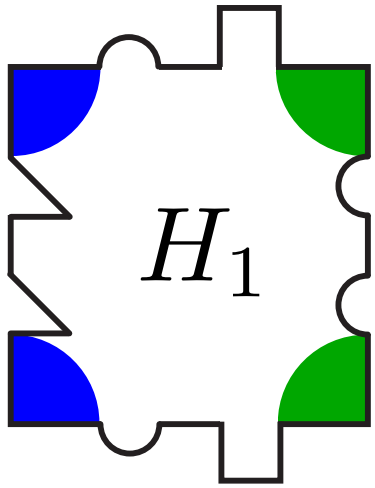

Figure 3.4: *This is a rotated version of tile* H_1 *in fig. 3.5. Each corner corresponds to the folding operator in that corner in fig. 3.3.*

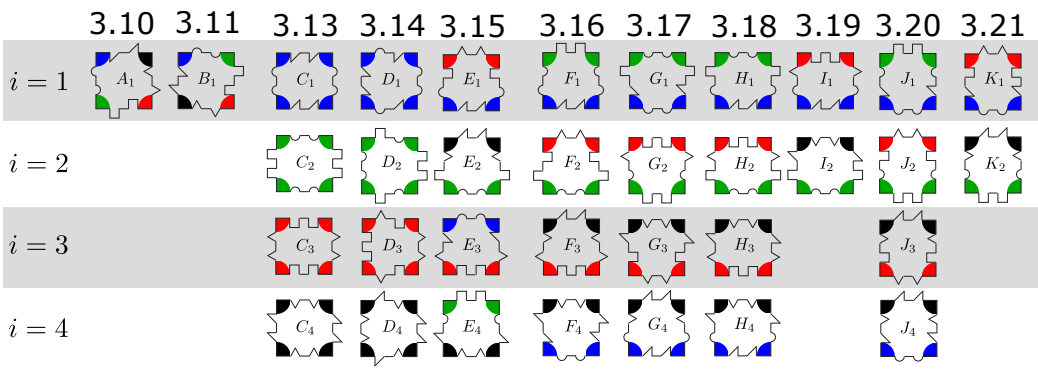

Figure 3.5: *A graphical representation of all the tiles generated by the loop conditions. The color coding is as follows: blue=a, green=b, red=c, black=d. The protrusions and indentations indicated in which direction the vertices are oriented (e.g. all vertices of tile A are oriented anticlockwise and all vertices of tile B are oriented clockwise).*

3.3 Tilings

We wish to connect our tiles together to create a large rigidly foldable sheet of connected quadrilaterals which we will call a *tiling*. Formally, a *tiling* of the plane is defined as a disjoint collection of open subsets of which the closures cover the entire plane [14]. We could use the interior of the shapes of the tiles in fig. 3.5 to fill the $\mathbb{R}^2$ plane and create a tiling.

However, this formal definition is not very useful for physical purposes, so we will regard a tiling as a way to fill an $m \times n$ grid with the tiles from fig. 3.5 fitting together as puzzle pieces, see fig. 3.7 for an example. The paper [12] tells us that an origami patterns is rigidly foldable if for a chosen assignment of the folding branches the loop conditions are satisfied for all tiles. Per construction of the tiles these conditions are at least satisfied for our tilings if all folding branches are the same. So, we can construct rigidly foldable tilings with multiple branches of motion (at least 2).

We can construct real 4-vertex meshes with quadrilateral faces from these tilings by choosing the angles a, b, c, d, which angles are supplemented, and the sizes of the quadrilaterals. These real meshes we call 4-vertex origami patterns. By using a 3d-printer we can physically create origami patterns corresponding to the tilings. We print the quadrilateral plates connected by hinges and show that they do indeed fold, fig. 3.6

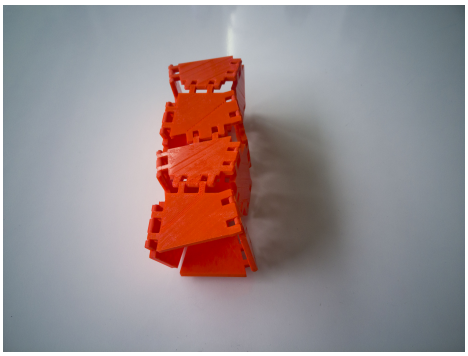

Figure 3.6: *A folded 3d-printed model of a tiling.*

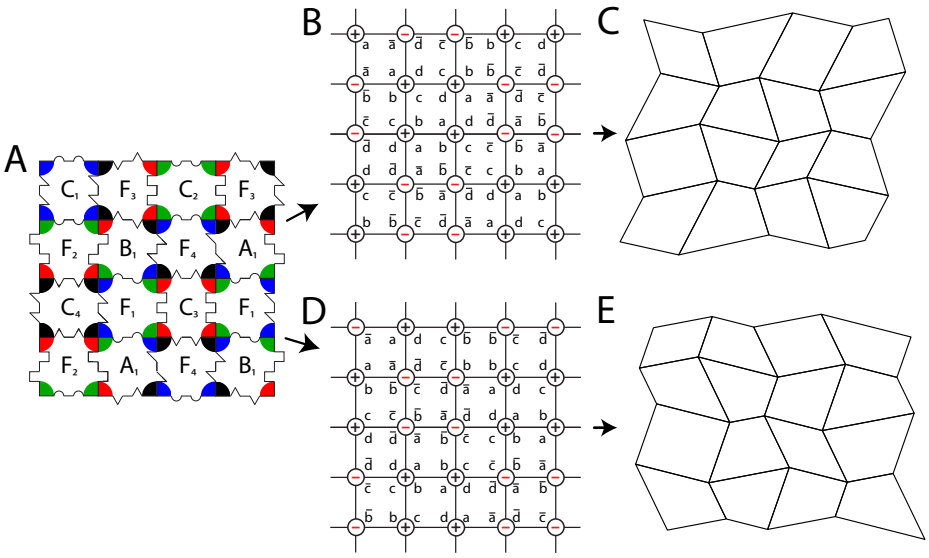

Figure 3.7: ***A*** *An example of how the tiles from fig. 3.5 can be used to form a general representation of a tiling.* ***B, D*** *Show how the supplemented angles can be assigned in different ways.* ***C, E*** *Correspond to two different real origami patterns represented by the same tiling.*

3.3.1 Compatible sides

We will state here explicitly which tiles we can fit together. If we can fit the schematic tiles it means we can create a real rigidly foldable origami pattern which is represented by these tiles, see the example in fig. 3.7. There are eight different combinations of tile sides which correspond to eq. 3.12. Of these eight different sides four correspond to $\hat{\rho}_{i+1,i}\hat{\rho}_{i,i+1}$. These four sides fit to the other four sides that correspond to $\hat{\rho}_{i+1,i+2}\hat{\rho}_{i+2,i+1}$, cf. fig. 3.8.

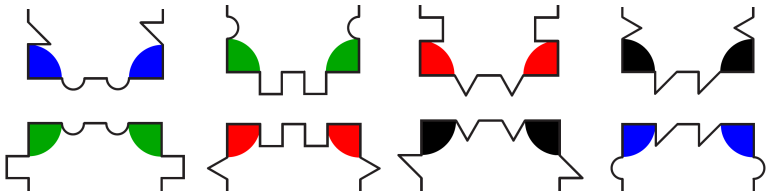

Figure 3.8: *In the top row the sides corresponding to operators $\hat{\rho}_{i+1,i}\hat{\rho}_{i,i+1}$ are given and in the bottom row the sides corresponding to operators $\hat{\rho}_{i+1,i+2}\hat{\rho}_{i+2,i+1}$.*

The sides corresponding to $\hat{\rho}_{i,i+1}\hat{\rho}_{i+1,i}$ are present in tiles $C_i, D_i, E_{i+2}, F_{i+3}, G_i, J_i, J_{i+3}$ and $K_{i(\mod 2)}$. The sides corresponding to $\hat{\rho}_{i+1,i+2}\hat{\rho}_{i+2,i+1}$ are present in tiles $C_{i+1}, D_{i+1}, E_{i+1}, F_{i+1}, G_i, H_i, H_{i+1}$ and $I_{i+1(\mod 2)}$. So, both of these types of sides occur 8 times in the set of tiles. Therefore, each tile fits to 8 other tiles on these sides.

There are four different sides that correspond to $\hat{\rho}_{i,i+1}\hat{\rho}_{i+1,i+2}$. They are present in tiles A_1 and F_i. These four sides fit only to themselves, fig. 3.9. Thus, each tile fits to 2 other tiles on these sides.

Similarly, there are four different sides that correspond to $\hat{\rho}_{i+2,i+1}\hat{\rho}_{i+1,i}$. They are present in tiles B_1 and F_i. These four sides fit only to themselves, fig. 3.10. Thus, each tile fits to 2 other tiles on these sides.

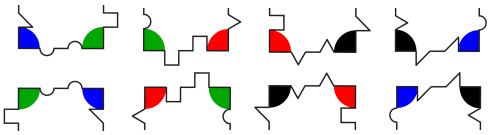

Figure 3.9: *The sides corresponding to operators $\hat{\rho}_{i,i+1}\hat{\rho}_{i+1,i+2}$ are given in both rows showing that they do fit to themselves.*

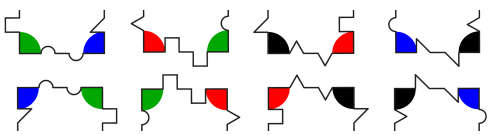

Figure 3.10: *The sides corresponding to operators $\hat{\rho}_{i+2,i+1}\hat{\rho}_{i+1,i}$ are given in both rows showing that they do fit to themselves.*

For all other tile sides there is only one other side that fits. For each tile that has two sides to which only one side fits there always is one single tile which fits on both these sides, see fig. 3.11 for an example. We will list all tiles that fit together on these sides.
for $i = 1, 2, 3, 4$:

- D_i fits to E_{i+3}.
- G_i fits to G_{i+2}.
- H_i fits to J_{i+1}.
- $I_{i(\mod 2)}$ fits to $K_{i+1(\mod 2)}$.

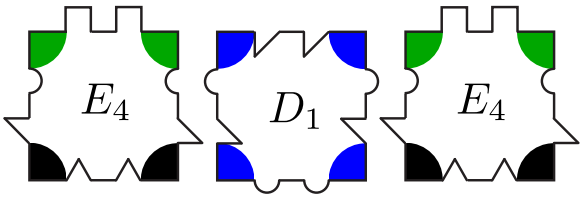

Figure 3.11: *An example of how two different sides of tile D_1 fit to two different sides of tile E_4.*

Chapter 4

4-Vertex Origami Patterns

4.1 Classification of the Configurations

Now that we have determined all possible tiles, section 3.2, we can use these to answer several questions about the tilings we can create with them:

- In how many ways can we combine the tiles from fig. 3.5 on a rectangular $m \times n$ grid?
- In how many ways can we assign the supplemented angles to these general tilings?
- In how many different ways can we fold each of these tilings?

To answer these questions we will first classify the different configurations into classes (see table 4.1). In the following sections we will add information on the supplemented angles and the folding branches into the tilings. Then we will see that some of the key properties of the tilings are different for these different classes.

We divide tilings into one of 4 main classes based on the presence of certain tiles. We consider *necessary* tilegroups and *optional* tilegroups for the different classes of tilings. A tiling belongs to a certain class if it has at least one tile of the necessary tilegroup of that class and further only tiles that are in its necessary or optional tilegroup. In this classification we can determine to which class a tiling belongs, using a decision tree, fig. 4.1.

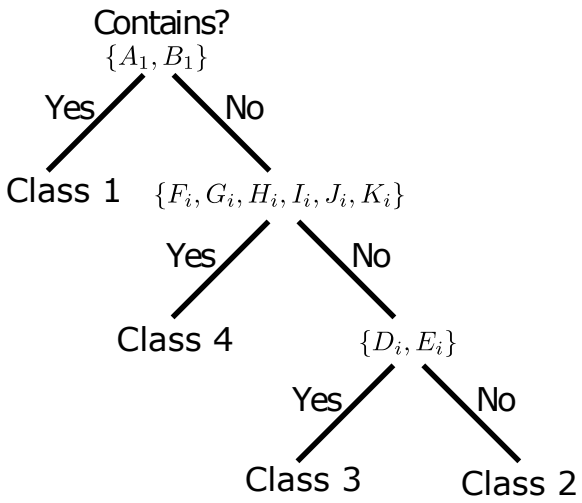

Figure 4.1: *A decision tree to determine to which class a tiling belongs. At each step the decision is made based on whether the tiling contains a certain tile.*

Class	Necessary tiles	Optional tiles
1	A_1, B_1	C_i, F_i
2	C_i	
3	D_i, E_i	C_i
4	$F_i, G_i, H_i, I_i, J_i, K_i$	C_i, D_i, E_i

Table 4.1: *Main classification of rigidly foldable tilings, based on which tile-groups they consist of.*

We subdivide some of these classes even further by introducing the notion of a tiling being *horizontally or vertically oriented*. We can place a combination of the tiles into a $m \times n$ grid, fig. 3.7. From the loop conditions we can see that for most tiles, except tiles A_1 and B_1, a composition of two of the folding operators associated to the corners of the tile may result in an identity operator, because of eq. 3.12. This means that the folds at the opposite sides of a tile often have the same folding angle, fig. 4.2. This leads us to the following definition.

Definition 4.1.1. A tiling is called *horizontally* (resp. *vertically*) *oriented* if on all tiles there is a $\pm \boldsymbol{I}$ operator between its horizontally (resp. vertically) opposite sides.

We introduce horizontal (resp. vertical) *folding lines* as lines of horizontal (resp. vertical) connected folds. For $m \times n$ internal tiles there are $m + 1$ horizontal and $n + 1$ vertical folding lines. Closely related to the

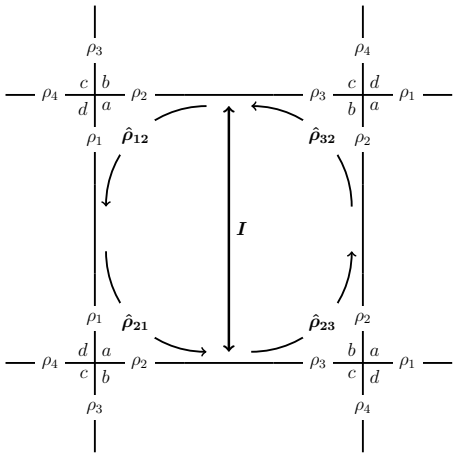

Figure 4.2: *An example showing the identity operator between opposite sides of a tile.*

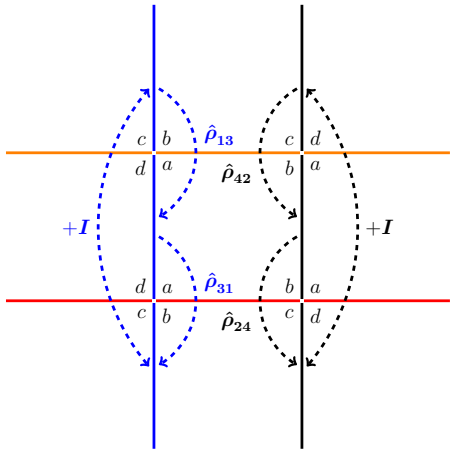

Figure 4.3: *An example showing the main vertical folding lines (black and blue). The horizontal folding lines are orange and red.*

orientation of a tiling we say that a tiling has horizontal (resp. vertical) *main folding lines* if there is a $+\boldsymbol{I}$ operator between every second fold on all horizontal (resp. vertical) folding lines, fig. 4.3. Per construction all horizontal (resp. vertically) oriented tilings have horizontal (resp. vertical) main folding lines.

- Class 1 configurations contain at least one tile A_1 or B_1. These tiles have four different folding angles at their sides, because these angles are equal to the 4 different folding angles that surround a single vertex. Therefore the tilings containing them are neither horizontally nor vertically oriented. However, since the vertices at each corner are rotated over 180 degrees with respect to their neighbours, there are both horizontal and vertical main folding lines.

- Class 2 configurations contain only tiles C_i. If all vertices have the same folding branch, there is a $\pm\boldsymbol{I}$ operator on all tiles between both pairs of opposite sides. Therefore these tilings can be both horizontally and vertically oriented.

- Class 3 configurations contain tiles D_i or E_i. These tiles have a $\pm\boldsymbol{I}$ operator between one of the pairs of opposite sides of the tiles.
  Let us assume we have one such tile which has a $\pm\boldsymbol{I}$ operator between its horizontally opposite sides. Then if we add a tile horizon-

tally next to this tile, it turns out using the loop conditions that there is only one possible tile that fits. This new tile is again a D_i or E_i tile that has a $\pm\boldsymbol{I}$ operator between its horizontally opposite sides. By repeating this argument we find that there is exactly one feasible row of tiles that arises from the original tile, that all have a $\pm\boldsymbol{I}$ operator between their horizontally opposite sides.

Next we add a tile to one of the vertical sides of the original tile. Let us say that the vertices connecting the tiles correspond to the folding operators $\hat{\boldsymbol{\rho}}_{ij}$ and $\hat{\boldsymbol{\rho}}_{ji}$ on the original tile. Then the vertices correspond to the folding operators $\hat{\boldsymbol{\rho}}_{i,j+2}$ and $\hat{\boldsymbol{\rho}}_{j+2,i}$ respectively. Then there is again a $\pm\boldsymbol{I}$ between the horizontally opposite sides on this tile. By repeating this argument we find that for all tiles in the same column as the original tile there is a $\pm\boldsymbol{I}$ operator between their horizontally opposite sides. Using these facts we conclude that the tiling is horizontally oriented.
This proves that we can properly subdivide the class 3 configurations into two subclasses of horizontally or vertically oriented tilings. However, for reasons that will become apparent when we add information on the supplemented angles for the origami patterns belonging to the tilings, we subdivide the configurations even further.

3-h-a: A horizontally oriented class 3 configuration with only tiles from either D_i or E_i in the same columns.

3-h-b: A horizontally oriented class 3 configuration with tiles from both D_i and E_i in the same columns.

3-v-a: A vertically oriented class 3 configuration with only tiles from either D_i or E_i in the same rows.

3-v-b: A vertically oriented class 3 configuration with tiles from both tilegroups D_i and E_i in the same rows.

- Class 4 configurations contain tiles F_i, G_i, H_i, I_i, J_i or K_i. Starting from one such a tile we can use the exact same reasoning as we did for class 3 configurations. Thus, we also arrive at a subdivision for the class 4 configuration into two subclasses,

4-h: A horizontally oriented class 4 configuration, and,

4-v: A vertically oriented class 4 configuration.

4.2 Counting the Configurations

4.2.1 Amount of Tilings

Now that we have divided the tiles into classes of configurations, we wish to count how many of these configurations there are. First we will simply count the amount of configurations of $m \times n$ interior tiles for each class using the set of 34 tiles.

First we observe an interesting property of the tilings

Lemma 4.2.1. *If there are 3 tiles lying connected in a L-shape, then there is a unique tile which fits into the corner.*

Proof. We checked this by going over all possible combinations of tiles. We can use this for when we know one row and one column in the tiling to uniquely determine the rest of the tiling. □

Class 1 configurations
Within class 1 configurations exactly two tiles fit to each side of any other tile. There has to be a tile A_1 or B_1 in the tiling so we start by looking at such a tile. We look at the first tile A_1 or B_1 we encounter when we check each position in the grid from left to right row after row. There are 2 such tiles, which can be rotated in 4 different ways giving us 8 options for this tile. When we have found this tile, all tiles in the same column above this tile can only be F tiles, since they were not A_1 or B_1 and they do have to fit to them. The same holds true for all tiles in the same row to the left. For each tile in the same column below, and each tile in the same row to the right of this first encountered tile, there are two possible fitting tiles. The rest of the tiles can be only found in one way, since they are enclosed both horizontally and vertically.

Thus, summing over the first position where we encounter a tile A_1 or B_1, say position (i, j), times the number of possible tiles on this position times the number of possible tiles to the right, 2^{n-j} and below 2^{m-i} give us

$$8 \sum_{i=1}^{m} \sum_{j=1}^{n} 2^{m-i+n-j} = 8(2^m - 1)(2^n - 1) \tag{4.1}$$

possible class 1 configurations.

Class 2 configurations
For class 2 configurations the entire tiling is determined is by the choice of

any one of the tiles. So there are 8 possible class 2 configurations regardless of the size of the tiling.

Class 3-h configurations
As stated in section 4.1, if a row contains a tile D_i or E_i then the entire row is uniquely determined. Thus, for the different amount of class 3-h configurations we only have to look at the amount of possibly different columns.

Once again we consider the first position where we encounter one of the necessary tiles, or row of tiles in this case. There are 8 of these, which can each be rotated in 2 ways giving us 16 possible tiles on this position. Above this tile there is each time only one allowed tile: C_i. Below this tile there are 3 allowed tiles each time. Thus, summing over the first position we can encounter a tile in tilegroup D_i or E_i times the number of different possible tiles on this position times the number of possible tiles below 3^{m-i} give us

$$16\sum_{i=1}^{m} 3^{m-i} = 8(3^m - 1) \tag{4.2}$$

possible class 3-h configurations.

For class 3-h-a configurations, there are only two allowed tiles on each tile below the first encountered tile D or E, giving us

$$16\sum_{i=1}^{m} 2^{m-i} = 16(2^m - 1) \tag{4.3}$$

possible class 3-h-a configurations.

From this we can also conclude, that there are

$$8(3^m - 1) - 16(2^m - 1) \tag{4.4}$$

possible class 3-h-b configurations.

Class 3-v configurations
From symmetry reasons, it follows that there are

$$16\sum_{j=1}^{n} 3^{n-j} = 8(3^n - 1) \tag{4.5}$$

possible class 3-v configurations,

$$16\sum_{j=1}^{n} 2^{n-j} = 16(2^n - 1) \tag{4.6}$$

class 3-v-a configurations and

$$8(3^n - 1) - 16(2^n - 1) \tag{4.7}$$

possible class 3-v-b configurations.

Class 4-h configurations
Similarly to class 3-h configurations, an entire row is uniquely determined if it contains a tile F_i, G_i, H_i, I_i, J_i or K_i. So, we only have to look at the different amount of class 4-h configurations for a single column.

There are 20 different tiles in F_i, G_i, H_i, I_i, J_i and K_i, each of which can be rotated in 2 ways such that the folding operators which commute to $\pm I$ lie on the same horizontal side of the tile.

Suppose we add a tile to the vertical side below the original tile. The folding operators on the vertices again have to commute to identity. So, the folding operators on the opposite side of the new tile have to be the identity. This gives 8 possible tiles. If we do not want the tiles to be in F_i, G_i, H_i, I_i, J_i and K_i, this gives 3 possibilities: C_i, D_i or E_i.

Once we have a tile of which two folding operators on one side commute to identity and a third folding operator is given the last folding operator has to commute to identity with this third operator. This means that a tile in a horizontally (resp. vertically) oriented tiling is completely determined by the two vertically (resp. horizontally) adjacent tiles.

Now we look at the highest tile in the first column in which we encounter a tile F_i, G_i, H_i, I_i, J_i and K_i. Say this tile is in row i. There are each time 8 possibilities, section 3.3.1, for each adjacent row below, 8^{m-i} in total, and 3 possibilities, C_i, D_i or E_i for each row above , 3^{i-1} in total. Summing over the first position at which we encounter the specified tile, gives us

$$40 \sum_{i=1}^{m} 8^{m-i} 3^{i-1} = 8(8^m - 3^m) \tag{4.8}$$

class 4-h configurations.

Class 4-v configurations
From symmetry reasons it follows that the amount of class 4-v configurations is

$$40 \sum_{j=1}^{n} 8^{n-i} 3^{n-1} = 8(8^n - 3^n). \tag{4.9}$$

Total configurations
Adding all these expressions together we find a total amount of configurations of

$$8(8^m - 2^m) + 8(8^n - 2^n) + 8 \cdot 2^{m+n}. \tag{4.10}$$

4.2.2 Amount of Origami Patterns

Next we will give the amount of valid origami patterns for each tiling by counting the number of ways to assign the supplemented angles. Strictly speaking assigning the supplemented angles still does not uniquely determine the origami pattern of a tiling, since the size of the quadrilaterals can still be varied. It does, however, uniquely determine the sign of the folding angles, once the folding branches are chosen. When the sector angles a, b, c, d of the single vertex are also chosen, the folding angles are completely determined. When assigning the supplemented angles we are limited by one trivial requirement. Namely, the sum of the sector angles in a single tile has to be 2π.

Class 1 configurations
We once again again look at a necessary tile A_1 or B_1. This is a generic quadrilateral. Thus either it has sector angles a, b, c and d, or it has sector angles $\bar{a}, \bar{b}, \bar{c}$ and $\bar{d}$. The horizontally and vertically adjacent tiles now have two different sector angles that are both either supplemented or not. Since the sum of the angles of this tile is 2π, the angles on the opposite of these tiles have to be supplemented both or not. Which of these holds follows, from the fact that A_1 and B_1 tiles have 0 or 4 supplemented angles and F_i tiles have 2. The same holds true for tiles on the opposite sides of the adjacent tiles. Repeating this argument gives that the only choice for supplemented angles in the entire row and column of this tile follows from the choice of supplemented angles for this particular tile. All other angles can be found by knowing that a tile always has an even number of supplemented angles. Additionally, if a tile is both horizontally and vertically enclosed by other tiles we already know three of its angles. This gives us 2 possible ways to assign supplemented for class 1 configurations.

Class 2 configurations
Suppose there is a tile with its supplemented angles the same along the vertical sides of the tile. Then the supplemented angles of the entire row

are determined. If we search for this row downwards, there are two possible ways to assign the supplemented angles on each lower row and one way on each higher row. This yields

$$2\sum_{i=1}^{m} 2^{m-i} = 2^{m+1} - 2 \tag{4.11}$$

possible assignments for supplemented angles. Analogously we find

$$2\sum_{j=1}^{n} 2^{n-j} = 2^{n+1} - 2 \tag{4.12}$$

possible assignments, if we assume that there is a tile with its supplemented angles along the horizontal sides.

There is also the possibility of all the supplemented angles being assigned to diagonally opposite angles giving us an extra 2 options. This means that in total there are

$$2^{m+1} + 2^{n+1} - 2 \tag{4.13}$$

ways to assign the supplemented angles for class 2 configurations.

Class 3-h configurations

Tiles D_i are on two opposite sides connected to tiles E_i and vice versa. Hence, there will always be a tile of tilegroup D_i if the configuration has at least two columns.

We use a similar approach as for class 2 configurations. Suppose there is a tile C_i or D_i with its supplemented angles the same along the vertical sides of the tile then the supplemented angles of the entire row are determined. If we start looking for this row from above to below, there are two possible ways to assign supplemented angles on each lower row and 1 way on each higher row. Giving

$$2\sum_{i=1}^{m} 2^{m-i} = 2^{m+1} - 2 \tag{4.14}$$

possible assignments for supplemented angles. Furthermore, suppose there is a column with only tiles C_i and D_i. Then we assume that on all tiles in this column the supplemented angles are assigned along the horizontal sides of the tiles. For the adjacent column there is only one option, since it contains tiles in tilegroup E_i. For the next column there are two options again, since it only contains tiles from tilegroups C_i and D_i. The amount

of valid assignments in this way depends on the amount of columns with only tiles in C_i and D_i. There are two possibilities in the case of an odd amount of columns

$$2\sum_{j=1}^{\lfloor \frac{n}{2} \rfloor} 2^{\lfloor \frac{n}{2} \rfloor - j} = 2^{\lfloor \frac{n}{2} \rfloor + 1} - 2, \text{ or} \tag{4.15}$$

$$2\sum_{j=1}^{\lceil \frac{n}{2} \rceil} 2^{\lceil \frac{n}{2} \rceil - j} = 2^{\lceil \frac{n}{2} \rceil + 1} - 2. \tag{4.16}$$

There is also the possibility of all the supplemented angles being assigned to diagonally opposite angles. This gives us two extra options. This means that in total there are

$$2^{m+1} \tag{4.17}$$

ways of assigning supplemented angles for class 3-h-b configurations and

$$2^{m+1} + 2^{\lfloor \frac{n}{2} \rfloor + 1} - 2, \text{ or} \tag{4.18}$$

$$2^{m+1} + 2^{\lceil \frac{n}{2} \rceil + 1} - 2 \tag{4.19}$$

for class 3-h-a configurations.

Class 3-v configurations
From symmetry reasons it follows that there are

$$2^{n+1} \tag{4.20}$$

ways of assigning supplemented angles for class 3-v-b configurations and

$$2^{n+1} + 2^{\lfloor \frac{m}{2} \rfloor + 1} - 2, \text{ or} \tag{4.21}$$

$$2^{n+1} + 2^{\lceil \frac{m}{2} \rceil + 1} - 2 \tag{4.22}$$

for class 3-v-a configurations.

Class 4-h configurations
Suppose there is a tile with its supplemented angles the same along the vertical sides of the tile. Then, the supplemented angles of the entire row are determined. If we search downwards for this row, we find two possible ways to assign supplemented angles on each lower row and one way on each higher row. This yields

$$2\sum_{i=1}^{m} 2^{m-i} = 2^{m+1} - 2 \tag{4.23}$$

possible assignments for supplemented angles. There is also the possibility that all diagonally opposite sector angles are supplemented. We find a total of

$$2^{m+1} \tag{4.24}$$

possible assignments of the supplemented angles.

Class 4-v configurations
From symmetry reasons it follows that there are

$$2^{n+1} \tag{4.25}$$

ways of assigning supplemented angles.

Total amount of configurations
If we combine the results from this section with those from the previous, we can find an expression for the amount of realizations of tilings we can make

$$\begin{aligned} 16(16^m + 16^n + (2^m - 1)(2^{\lfloor \frac{n}{2} \rfloor} + 2^{\lceil \frac{n}{2} \rceil} + 2^n - 2) + \\ (2^n - 1)(2^{\lfloor \frac{m}{2} \rfloor} + 2^{\lceil \frac{m}{2} \rceil} + 2^m - 2) - 2^{m+n}). \end{aligned} \tag{4.26}$$

4.2.3 Remarks

Some of the tilings and the amount of origami patterns per tiling we found, may be doubly counted. We can prevent this by demanding that a is the unique angle and that $b < d$. We also require that the upper left vertex in the tiling is unsupplemented. This does mean the amount of possible origami patterns per tiling is halved.

We can also create many more foldable patterns in a similar manner than only those that we constructed using a single generic 4-vertex, its supplement, and its mirror image. This is possible by using a different generic 4-vertex with angles a', b', c', d' and its supplement and mirror image along one of the main folding line in class 2, 3 or 4 configurations. These origami patterns contain the more general linear compound type Kokotsakis quadrilaterals discussed in section 3.1.

4.3 Folding Branches

In the previous sections we determined many different tilings that are rigidly foldable using the tiles represented by folding operators. However,

using some brute force calculations combining the equations of many single Kokotsakis quadrilaterals using the equations from [13] we could have also found these same tilings. One of the additional benefits of having used our method is, that we can not only say whether a tiling will rigidly fold, but also conclude in how many different ways it will.

In [15] it is described that a tiling using only generic quadrilaterals, the tiles A_1 and B_1, produces a tiling that can fold into a cylindrical shape along both the horizontal and vertical direction. In this section we will study in how many ways a tiling can fold and in the next chapter 5 we will investigate the shapes they can produce.

To find out in how many ways a tiling can fold, we simply count how many different ways there are of assigning folding branches to the vertices. The folding branches must be assigned such that combining the four folding operators corresponding to the vertices of one single tile still results in an identity operator. To that end we note that folding operators commute to identity in eqs. 3.10,3.11, 3.13–3.21 if and only if they have the same folding branch e.g. $\hat{\boldsymbol{\rho}}^{\boldsymbol{I}}_{ij}\hat{\boldsymbol{\rho}}^{\boldsymbol{I}}_{ji} = \boldsymbol{I}$, but $\hat{\boldsymbol{\rho}}^{\boldsymbol{I}}_{ij}\hat{\boldsymbol{\rho}}^{\boldsymbol{II}}_{ji} \neq \boldsymbol{I}$.

Class 1 configurations

We start by looking at a tile A_1 or B_1. All four vertices of this tile have to have the same folding branch. The horizontally and vertically adjacent tiles have on their adjoining side two folding operators that do not commute to identity. If they have the same folding branch, the vertices lying on the opposite side of the tile both have to have the same folding branch to remain rigidly foldable. This property propagates across the entire column or row. By repeating this argument it becomes clear that the only option for folding branches in the entire row and column of this A_1 or B_1 tile is the choice of all vertices having the same folding branch. So the total amount of ways to assign the folding branches equals

$$2. \tag{4.27}$$

Class 2 configurations

We start by looking at the upper left tile. If this tile has the same folding branches on the vertices along the vertical sides of the tile such that the folding operators along the vertical side commute to $\pm\boldsymbol{I}$, then the same has to be true for all tiles to the right. Assume there is one tile whre on the left and right side the folding branches are different. Just as in the case where we counted the assignment of the supplemented angles , we can now sum over the first position from the left where we encounter such a

tile. This gives us

$$2\sum_{i=1}^{m} 2^{m-1-i} = 2^{m+1} - 2 \tag{4.28}$$

options of assigning the folding branches. Analogously we find

$$2\sum_{j=1}^{n-1} 2^{n-1-j} = 2^{n+1} - 2 \tag{4.29}$$

if the folding branches of the vertices along the horizontal sides of the tile are the same and there is a tile where the folding branch along the left side is different from the folding branch along the right side.

There is also the possibility of all vertices having the same folding branch. So we find a total of

$$2^{m+1} + 2^{n+1} - 2 \tag{4.30}$$

ways of assigning the folding branches.

Class 3-h and 4-h configurations
Look at the left most tile of the highest row of tiles that is not a C_i tile. Only the vertices lying on the same horizontal sides of the tiles can commute to identity as in eq. 3.12. So they have to be assigned the same folding branch. The tile to the right has on its left side again two folding operators that do not commute to identity. So the vertices lying along the horizontal sides of the tile need to have the same folding branch to remain rigidly foldable. The same goes for the tile to the right of this tile. By repeating this argument it becomes clear that all vertices lying in one row have the same folding branch.

The tile below the tile we considered first has the folding operators on the vertices on its upper side commute to identity. Hence, the folding operators on the vertices on its lower side should commute to identity too. This means they should have the same folding branch. There are 2 options to choose from. By repeating this argument we find that there is a total amount of ways to assign the folding branches of

$$2^{m+1}. \tag{4.31}$$

Class 3-v and 4-v configurations
From symmetry it follows that there are

$$2^{n+1} \tag{4.32}$$

ways of assigning the folding branches.

Chapter 5

Mountain-Valley Patterns

In section 4.2 we studied the possible configurations extensively and in section 4.3 we derived the amount of possible assignments of folding branches given the class of the configuration.

In this chapter we will take the first small step towards designing 3-dimensional structures using origami patterns. Since given an operator $\hat{\boldsymbol{\rho}}_{ij}^{I/II}$ the sign of $\hat{\boldsymbol{\rho}}_{ij}^{I/II}\rho$ is completely dependent on the sign of ρ and the assignment of the supplemented angles, we know that each of these assignments of folding branches corresponds to a unique *mountain-valley pattern* and its opposite for a given configuration of tiles. However, the mountain-valley patterns are not unique for multiple different tilings.

Definition 5.0.1. Let a crease pattern $C = (W, E)$ be given, with W the internal vertices and E the folds of an origami pattern, including the edges between the outer quadrilaterals. A *mountain-valley pattern* is a function $\mu : E \to \{M, V\}$ that indicates which folds are mountains and which are valleys.

The folds E of the crease pattern $C = (W, E)$ are also known as *creases*. The question that we will study in this chapter is: which mountain-valley patterns can we create using a generic quadrilateral tiling? When we know this, we will look for an explicit way to construct a tiling for a valid given mountain-valley pattern. Finally, we will also consider so-called forcing sets. These will tell us something about how to force a tiling with multiple possible mountain-valley patterns to fold accordingly to a specific one.

5.1 Requirements on Mountain-Valley Patterns

As stated in section 2.1, in a single 4-vertex one fold is folded in the other direction than the other three (3-1 rule).

Requiring this to be true for all vertices, we already know an upper bound for the amount of mountain-valley patterns for a tiling placed on a $m \times n$ grid, namely $2^{(m+2)(n+2)-1}$ [16].

However, when we combine multiple vertices, new rules come in to play that were not yet there for single vertices.

Remark 5.1.1. As discussed in section 4.1, for horizontally (resp. vertically) oriented tilings, we see that along all lines of connected horizontal (resp. vertical) folds either the folding operators $\hat{\boldsymbol{\rho}}_{\mathbf{13}}$ and $\hat{\boldsymbol{\rho}}_{\mathbf{31}}$ or $\hat{\boldsymbol{\rho}}_{\mathbf{24}}$ and $\hat{\boldsymbol{\rho}}_{\mathbf{42}}$ alternate, giving a $+\boldsymbol{I}$ operator between every second fold on these lines, fig. 4.3.

This is independent of the assignment of supplemented angles,since supplementation of the sector angles has no impact on the folding operators $\hat{\boldsymbol{\rho}}_{\mathbf{13}}$, $\hat{\boldsymbol{\rho}}_{\mathbf{31}}$, $\hat{\boldsymbol{\rho}}_{\mathbf{24}}$ and $\hat{\boldsymbol{\rho}}_{\mathbf{42}}$. For class 1 tilings the lines of connected folds in both directions have this $+\boldsymbol{I}$ operator between every second fold. These lines have been called *main folding lines*.

The folding lines perpendicular to the main folding lines are called *secondary folding lines*.
Along these main folding lines there are repeating mountain-valley patterns with period 2. So, each main folding line has at most 4 possible mountain-valley assignments. Now there at most 2 options left for each secondary folding line. If the sign of one fold on a secondary folding line is chosen, the rest of the folds on this line can be determined using the 3-1 rule.

This all gives us a new upper bound of $2^{m+n+3}(2^m + 2^n)$, which is much smaller than the previous upper bound. We can make it even smaller. To this end we need to take a much more detailed look into the mountain-valley patterns.

Definition 5.1.2. A tile is said to lie on an odd-checkered position, when it either lies on an odd column and an odd row or an even column and an even row.

Similarly we a tile is said to lie on an even-checkered position, when it either lies on an even column and an odd row or on an odd column and an even row. See example in fig. 5.1.

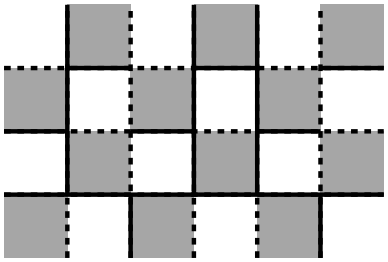

Figure 5.1: *A mountain-valley pattern, where the solid lines are mountains and the dashed lines are valleys. The odd checks are white and the even checks are gray. This pattern has main horizontal folding lines.*

Definition 5.1.3. A tile is said to contain a *critical motif* when both pairs of opposite sides have the same folding direction (i.e. both mountain or both valley). See fig. 5.2 for an example.

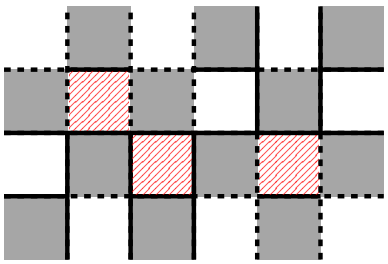

Figure 5.2: *A mountain-valley pattern, where the critical motifs are indicated by hatched red lines.*

Remark 5.1.4. Tiles A_1 and B_1 cannot have a critical motif.

Since the 4 folding angles of the folds at the sides of the tiles are the same as the folding angles around a single vertex, exactly one of the sides has a folding angle with opposite sign.

Lemma 5.1.5. *A critical motif can only occur on tiles that consist of two identical sector angles along one main folding line and their supplemented angles on the other side of the tile. These sector angles do not correspond to the unique plate or the anti-unique plate.*

Proof. Between two parallel secondary folding lines next to each other there always is a $\pm\boldsymbol{I}$ operator by eq. 3.12 (except for class 1 configurations with tiles A_1 and B_1, but they do not contain a critical motif) and so

in the case of a critical tile there is a $+\boldsymbol{I}$ operator, so both the supplemented angles have to lie along one main folding line. Since the sector angles of a single tile sum to 2π, the critical tile itself now has to consist of two identical sector angles lying along one of the main folding lines and two supplemented sector angles lying along the other (an isosceles trapezoid).

If one of the sector angles corresponds to a unique or anti-unique plate, then the folds around it have different (resp. same) sign. Its diagonally opposite sector angle in the tile, which is its supplement, is the anti-unique (resp. unique) angle. So, the folds around it have the same (resp. opposite) sign. Thus, this can not result in a critical tile. □

Lemma 5.1.6. *If a configuration contains a critical tile then all tiles on odd-checkered positions consist only of sector angles $a, c, \bar{a}, \bar{c}$ and all tiles on even-checkered positions consist only of sector angles $b, d, \bar{b}, \bar{d}$ or vice versa.*

Proof. We look at a critical motif and without loss of generality we assume that the tile it lies on consists of angles b and $\bar{b}$ and that the main folding lines are vertical.

The adjacent side of a horizontally adjoining tile has one of the angles $a, \bar{a}, c$ or $\bar{c}$ twice. Thus, the angles on the other side of this tile are both $\bar{a}, a, \bar{c}$ or c respectively. For the next horizontally adjoining tile the same applies, but with angles $b, \bar{b}, d$ or $\bar{d}$. Repeating this, implies the validity of the lemma for all tiles on the same row as the critical motif.

The adjacent side of a vertically adjoining tile has a combination of angles of $a, \bar{a}, c, \bar{c}$. Since there has to be a $\pm\boldsymbol{I}$ operator between every second fold along the main folding line, the other angles also have to be a combination of $a, \bar{a}, c, \bar{c}$. For the next adjoining tile the same applies, but with angles $b, \bar{b}, d, \bar{d}$. Repeating this, implies the validity of the lemma for all tiles lying in the same column as the critical motif.

For a tile enclosed on two sides by tiles with only angles $a, c, \bar{a}, \bar{c}$ three of its sector angles are within $b, d, \bar{b}, \bar{d}$. Since the sum of sector angles of a tile is 2π, the fourth angle also has to be within $b, d, \bar{b}, \bar{d}$. The analogous applies to a tile enclosed by tiles with only angles $b, d, \bar{b}, \bar{d}$.

□

Theorem 5.1.1. *A mountain-valley pattern is realizable using a generic quadrilateral tiling if and only if it has in at least one direction lines of connected folds where each second fold has the same mountain or valley assignment and if all critical motifs (if there are any) lie on either odd- or even-checkered positions.*

Proof. $\Rightarrow$ If a pattern is realizable there have to be main folding lines in at least one direction. For all lines of connected folds in this direction every second fold has the same mountain or valley assignment.

By lemma 5.1.5 all critical tiles are made up of angles that do not correspond to unique or anti-unique plates. By lemma 5.1.6 these angles are only contained in tiles that either all lie on odd-checkered or on even-checkered positions.

$\Leftarrow$: We will be prove this by construction in section 5.2. □

5.2 From Mountain-Valley Patterns to Tilings

In this section we give a way to construct a tiling realizing all valid mountain-valley patterns. We assume a to be the unique angle.

1. Look for a suitable direction for the main folding lines by finding the direction in which the folding lines have a repeating base of MM, MV, VM or VV.

2. If there is an odd (resp. even) critical tile, we only use tiles C_2, C_4, D_2, D_4 on odd (resp.even) positions and C_1, C_3, E_1, E_3 on even (resp. odd) positions. If there is no critical tile we use the tiles as if there is an odd critical tile.

3. If two folds with opposite sign on two different main folding lines enclose a tile that does not contain unique or anti-unique sector angles, then lay tiles C_i between the two main folding lines in a suitable way. If the main folding lines follow the exact opposite mountain-valley pattern, then the folding branches along these lines are different, otherwise the folding branches are the same.

   If two folds with the same sign on two different main folding lines enclose a tile that does contain unique or anti-unique sector angles, then lay tiles D_2, D_4, E_1, E_3 between the two main folding lines in a suitable way. If the main folding lines follow the exact same mountain-valley pattern, then the folding branches along these lines are different, otherwise the folding branches are the same.

4. If two folds with opposite sign on two different secondary folding lines enclose a tile, then the supplemented angles of tiles enclosed by these secondary folding lines should be assigned to diagonally opposite corners of the tile.

   If two folds with the same sign on two different secondary folding lines enclose a tile, then the supplemented angles of tiles enclosed by these secondary folding lines should be assigned, such that vertices

along the same main folding line are both either supplemented or not.

5. We fill in the tiles and supplemented angles such that the top left vertex is not-supplemented and not-mirrored. Further, we make sure that the corner enclosed by one mountain and one valley fold that is allowed by the second step in this construction to be a C_1 or E_1 tile, also really is a C_1 or E_1 tile.

If it is possible to find a class 2 tiling for a mountain-valley pattern, this construction will give it. Otherwise we get a class 3 tiling.

5.3 Amount of Mountain-Valley Patterns

Now that we have the necessary and sufficient conditions for mountain-valley patterns, we can use them to count how many patterns there are possible.

Since every second fold on a main folding line has the same sign, the main folding lines can have 4 different repeating bases MM, MV, VM or VV. Because of the 3-1 rule, two secondary folding lines can follow a pattern similar or opposite to each other.

This result in 4 different ways in which two adjacent folding lines can relate, which we call types.

1. They follow the exact same mountain-valley pattern.

2. They follow the exact opposite mountain-valley pattern.

3. On odd tiles the opposite sides have the same fold (i.e. they are either both mountains or they are both valleys) and on even tiles the opposite sides have a different fold.

4. On even tiles the opposite sides have the same fold and on odd tiles the opposite sides have a different fold.

The folds around a single vertex and all relations between the folding lines determine a mountain-valley pattern. Not all combinations of relations between adjacent folding lines are allowed.

- If a column of tiles is of type 3 or type 4, then none of the rows can be so too and vice versa.

- By theorem 5.1.1, there are no critical motifs on both odd-checkered and even-checkered positions. We get odd-checkered critical motifs for any of the following combinations:
  - An odd row of tiles of type 1 or 3 and an odd column of tiles of type 1 or 3.
  - An even row of tiles of type 1 or 3 and an even column of tiles of type 1 or 3.

  We get even-checkered critical motifs for any of the following combinations:
  - An odd row of tiles of type 1 or 4 and an even column of tiles of type 1 or 4.
  - An even row of tiles of type 1 or 4 and an odd column of tiles of type 1 or 4.

We use these rules to calculate the following table 5.1 with the number of feasible combinations, $COMB(i, j, k, l)$, of different types of rows and columns of tiles in which i is the number of different types of different odd rows, j the number of different types of even rows, k the number of different types of odd columns and l the number of different types of even columns.

The amount of different ways to distribute k different types of rows (or columns) among n total rows (or columns) such that each type occurs at least once is given by the Stirling numbers of the second kind [17],

$$S(n,k) = \frac{1}{k!}\sum_{j=0}^{k}(-1)^{(k-j)}\binom{k}{j}j^n. \tag{5.1}$$

When we wish to distinguish between the different types of rows we have to multiply by a factor $k!$

$$S'(n,k) = k! \cdot S(n,k). \tag{5.2}$$

The folds around a single vertex give 8 different folding patterns. So, we now have together with all relations between the folds all necessary information to find an expression for the total amount of different allowed folding patterns of a $m \times n$ tiling

	i	1					2				3				4			
k	l \j	0	1	2	3	4	1	2	3	4	1	2	3	4	1	2	3	4
1	0	12	36	42	24	6	42	49	28	7	24	28	16	4	6	7	4	1
	1	36	83	71	32	8	71	66	32	8	32	32	16	4	8	8	4	1
	2	42	71	35	8	2	35	17	4	1	8	4	0	0	2	1	0	0
	3	24	32	8	0	0	8	0	0	0	0	0	0	0	0	0	0	0
	4	6	8	2	0	0	2	0	0	0	0	0	0	0	0	0	0	0
2	1	42	71	35	8	2	35	17	4	1	8	4	0	0	2	1	0	0
	2	49	66	17	0	0	17	4	0	0	0	0	0	0	0	0	0	0
	3	28	32	4	0	0	4	0	0	0	0	0	0	0	0	0	0	0
	4	7	8	1	0	0	1	0	0	0	0	0	0	0	0	0	0	0
3	1	24	32	8	0	0	8	0	0	0	0	0	0	0	0	0	0	0
	2	28	32	4	0	0	4	0	0	0	0	0	0	0	0	0	0	0
	3	16	16	0	0	0	0	0	0	0	0	0	0	0	0	0	0	0
	4	4	4	0	0	0	0	0	0	0	0	0	0	0	0	0	0	0
4	1	6	8	2	0	0	2	0	0	0	0	0	0	0	0	0	0	0
	2	7	8	1	0	0	1	0	0	0	0	0	0	0	0	0	0	0
	3	4	4	0	0	0	0	0	0	0	0	0	0	0	0	0	0	0
	4	1	1	0	0	0	0	0	0	0	0	0	0	0	0	0	0	0

Table 5.1: *A table giving the values of $COMB(i,j,k,l)$. These were calculated using a python script.*

$$\sum 8 \cdot COMB(i,j,k,l) S'(\lceil \frac{m}{2} \rceil, i) S'(\lfloor \frac{m}{2} \rfloor, j) S'(\lceil \frac{n}{2} \rceil, k) S'(\lfloor \frac{n}{2} \rfloor, l). \tag{5.3}$$

The restrictions on the summation indices are given by

$$\begin{aligned} 1 \leq i \leq \min\{4, \lceil \frac{m}{2} \rceil\}, \\ \mathbb{1}(\lfloor \frac{m}{2} \rfloor \geq 1) \leq j \leq \min\{4, \lfloor \frac{m}{2} \rfloor\}, \\ 1 \leq k \leq \min\{4, \lceil \frac{n}{2} \rceil\}, \\ \mathbb{1}(\lfloor \frac{n}{2} \rfloor \geq 1) \leq l \leq \min\{4, \lfloor \frac{n}{2} \rfloor\}. \end{aligned} \tag{5.4}$$

5.4 Forcing Sets

In this section we will focus on forcing sets for generic 4-vertex tilings. A *Forcing set* is a subset $F \subset E$ of creases of the crease pattern $C(W,E)$, such

that the assignment of mountains or valleys to all other creases is uniquely determined. The study of forcing sets was first introduced in [18] and this paper serves as an inspiration for this entire section. First we give a formal definition of forcing sets.

Definition 5.4.1. Let $C(W, E))$ be a given crease pattern. A subset $F \subset E$ is a *forcing set* for a mountain-valley assignment $\mu : E \to \{M, V\}$ if there are no other mountain-valley assignments that agree on the restriction to F.

If this is true for all mountain-valley assignments μ, then F is called a *strong forcing set.*

Forcing sets are useful when we wish to fold an entire tiling by exerting force onto only a select number of folds. This way, we can create tilings that will seemingly fold themselves. It may be economically desirable to look for the minimum number of folds required in a forcing set.

Note that we do not impose a folding angle, but merely the sign of the folding angle.

In the case of the single 4-vertex we know that the folds around the unique fold always have the opposite sign and the folds around the anti-unique plate always have the same sign. This means that a set containing one of the folds around the unique plate and one of the folds around the anti-unique plate is a forcing set for the single 4-vertex.

Furthermore, when we know the folding branch of a vertex, only one fold is needed to determine the other folds. We look at an example of a class 4-h folding to see what this means for the forcing set.

Class 4 patterns

As we saw in section 4.1 there is always a $+\boldsymbol{I}$ operator between every second fold along a main folding line. So those folds uniquely determine each other and we colour them the same in figure 5.3. The other folds we colour by looking at the unique and anti-unique plates as for the single 4-vertex. Now we can get a forcing set by choosing one edge from each coloured subset of edges. These unique and anti-unique angles are at different positions for each tiling and choice of supplemented angles. Thus, the forcing sets must be determined for each individual tiling and assignment of supplemented angles.

Every second fold along the main folding line is in the same coloured set. Each colouredset with exception one of the sets on both of the outer main folding lines contains folds along two different folding lines. So, colouring this way leaves us for $m \times n$ tiles with $n + 2$ differently coloured subsets of edges. Since there are 2^{n+1} ways of assigning the folding branches,

see section 4.3, there are 2^{n+2} different mountain-valley patterns. Thus any set of edges created by choosing one edge from each colored subset is a (strong) forcing set of minimum size.

In the same way we can find that there are (strong) forcing sets of minimum size $m+2$ for type 4-v configurations.

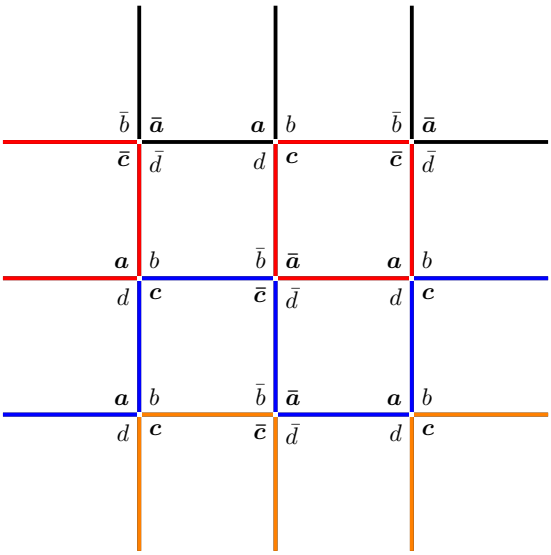

Figure 5.3: *An example of the (strong) forcing sets in a class 4-h tiling. The unique and anti-unique angles are bold. The different colours represent the subsets of edges of which each forcing set must contain at least one edge.*

Class 3 patterns

In the same way as for class 4 patterns, we can find that there are (strong) forcing sets of minimum size $n+2$ for type 3-h configurations and (strong) forcing sets of size $m+2$ for type 3-v configurations. These strong forcing sets look the same with at least every second fold along a main folding line in the same set.

Class 1 patterns

For type 1 configurations we have main folding lines in both directions. Thus between every second fold along the vertical (or horizontal) main folding lines there is a $+\boldsymbol{I}$ operator and they lie in the same set. We can determine to which coloured sets the other edges belong using the unique and anti-unique plates.

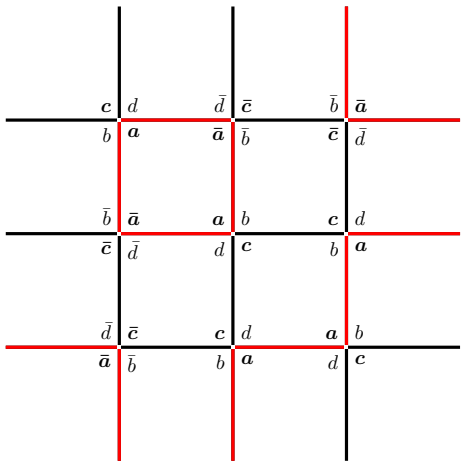

Figure 5.4: *An example of the (strong) forcing sets in a class 1 tiling. The unique and anti-unique angles are bold. The different colours represent the subsets of edges of which each forcing set must contain at least one edge.*

We see we have two differently coloured subsets of edges. Since there are 2 ways of assigning the folding branches, see section 4.3, there are 4 different mountain-valley patterns. Thus any set of edges created by choosing one edge from each coloured subset is a (strong) forcing set of minimum size.

Class 2 patterns

For class 2 configurations some things change. Forcing sets are no longer necessarily strong forcing sets too.

If the tiling is folded such that there are only horizontal (resp. vertical) main folding lines then the forcing subsets are similar to those for class 3-h or class 4-h (resp. class 3-v or 4-v) and they have minimum size $n+2$ (resp. $m+2$).

To create a strong forcing set, a set of folds must be found that is a forcing set both when there are horizontal and when there are vertical main folding lines. We can create a a strong forcing set by choosing one edge in each coloured subset for horizontal main folding lines and one edge in each coloured subset for vertical main folding lines. We need at least $\max(m+2, n+2)$ edges for this. Since there are $2^{m+1}+2^{n+1}-2$ ways of assigning the folding branches, see section 4.3, there are $2^{m+2}+2^{n+2}-4 > 2^{\max(m+2,n+2)}$ different mountain-valley patterns for $m, n \geq 1$. Thus any set of edges created this way is a strong forcing set of minimum size.

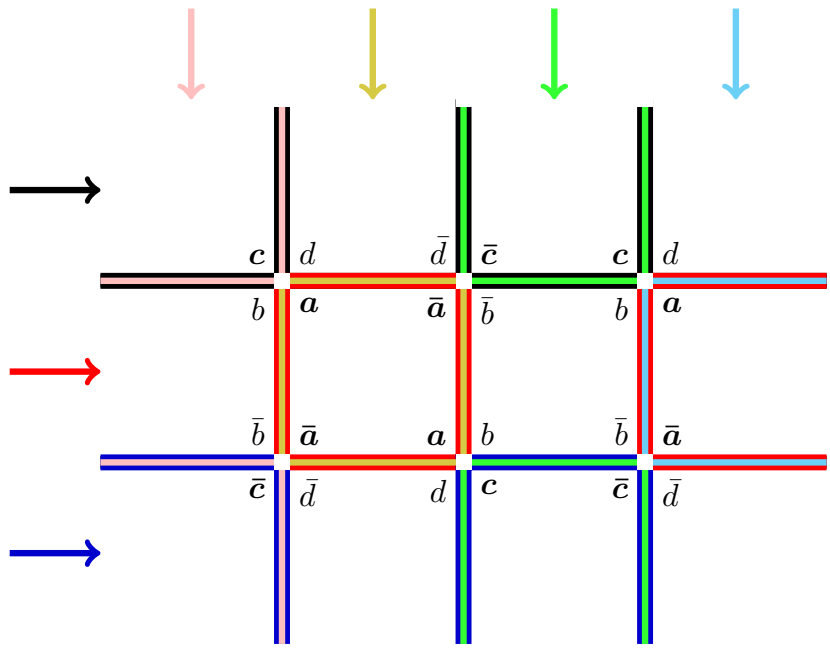

Figure 5.5: *An example of the (strong) forcing sets in a class 2 tiling. The unique and anti-unique angles are bold. The different colours with horizontal (resp. vertical) arrows represent the subsets of edges of which each forcing set must contain at least one edge for mountain valley patterns with only horizontal (resp. vertical) main folding lines. The coloured subsets are no longer disjoint.*

Chapter 6

Conclusion

6.1 Summary

Using a single generic 4-vertex, its supplement, and its mirror image, we designed a method to create an arbitrarily large rigidly foldable tiling. The combinatorial approach we used, has enabled us to design a single foldable schematic tiling and create many different foldable origami-patterns from it. We found according to which mountain-valley patterns these origami patterns can fold and even described a method for constructing an origami pattern which will fold according to a given mountain-valley pattern. Since we found that origami patterns have many different folded states, we also described how one could force an origami pattern to fold into a specific mountain-valley pattern.

6.2 Project description

In the van Hecke group there was an idea of how more schematic tilings could be used to describe the folding of a specific set of real origami patterns. The initial goal was mainly to find the number of different tilings and also the number of related origami patterns. We have been able to solve this completely. In addition, we have been able to characterize these tilings based on the individual tiles they are composed of.

During the course of the thesis we also decided to have a look at mountain-valley patterns. We found all mountain-valley patterns we could create using our tilings. We also described how to design specific origami patterns that fold according to a given mountain-valley pattern. Finally, we described the forcing sets for the origami patterns.

For chapter 2, where we discussed the single 4-vertex, and chapter 3, where we discussed rigidly foldable Kokotsakis quadrilaterals, most of the results we presented were already known, be it published or within the research group. Our own work in these chapters lies mainly in selecting and right information and showing how they relate to our research. This includes a thorough review of the sources and highlighting the most important and relevant facts. For example, while the relations between the folding angles in a single vertex are known, we could not find any source that used these relations to remark the similarity in folding behaviour between a 4-vertex and its supplement.

Chapter 4, where we described the rigidly foldable tilings and origami patterns we can create, is completely our own work and includes the results for our initial research goals.

Chapter 5, where we discussed mountain-valley patterns, is also completely our own work. The inspiration for studying these mountain-valley patterns came from several other research papers.

6.3 Discussion

We know that we can create even more foldable patterns than those that we constructed using a single generic 4-vertex, its supplement, and its mirror image. For example, by using different generic 4-vertices with their supplement and mirror images along each different horizontal or vertical lines of vertices. What we do not know is, if we described all foldable patterns with generic vertices that will fold in multiple different ways, included these slightly other patterns. Possibly, this can be checked by closer reviewing the recent work of Izmestiev [13] in section 3.1.

There is a possible problem we did not treat in this thesis and that is that in the folding of some large origami patterns, the plates may start intersecting one another. This occurs especially often when we have many type 1 columns or rows next to each other as in the Huffman-tiling [1]. We were allowed to ignore this problem since we just looked at some finite folding motion, not necessarily a large folding motion. The reason we did this, is mainly because it is a very difficult problem. In the case of an origami pattern with all flat-foldable vertices it has been shown that determining whether or not self-intersection occurs is an NP-hard problem [19]. However, if someone wishes to design 3-dimensional structures from the patterns we described, it may be necessary to take this into consideration.

An interesting discovery that was made during this research is, that it is possible to create multistable origami patterns, that have several stable states in which there is no strain on any of the quadrilateral plates. We managed to get these multistable tilings by the following procedure. We first take 3×3 quadrilaterals and remove a quadrilateral on one of the corners. Now we have a system with 8 quadrilaterals which is no longer overconstrained and has one degree of freedom. We fold this system and fit a folded flat vertex onto the corner where the quadrilateral was removed. For these systems now both the folded state to which they were fitted, the one with opposite folding angles, and the unfolded state are stable. We do not know if this method always works, but we have found several examples where it did. Further research into this may be interesting.

Acknowledgments

First I would like to thank MSc. Peter Dieleman for his guidance throughout the entire period I spent working on this thesis, for always being available to give me feedback on my work and also for providing several of the figures in this thesis. I would also like to thank dr. Floske Spieksma for her supervision and feedback on the thesis, and prof. dr. Martin van Hecke for allowing me to write my thesis in his research group and his supervision.

References

[1] D. A. Huffman, "Curvature and creases: A primer on paper," *IEEE Transactions on computers*, no. 10, pp. 1010–1019, 1976.

[2] K. Miura, "Method of packaging and deployment of large membranes in space," *The Institute of Space and Astronautical Science report*, vol. 618, pp. 1–9, 1985.

[3] P. T. Barreto, "Lines meeting on a surface: The "mars" paperfolding," in *Proceedings of the 2nd International Meeting of Origami Science and Scientific Origami*, pp. 323–331, 1997.

[4] T. Tachi, "Rigid folding of periodic origami tessellations," *Origami^6: I. Mathematics*, p. 97, 2015.

[5] T. Tachi, "Generalization of rigid foldable quadrilateral mesh origami," in *Symposium of the International Association for Shell and Spatial Structures (50th. 2009. Valencia). Evolution and Trends in Design, Analysis and Construction of Shell and Spatial Structures: Proceedings*, Editorial Universitat Politècnica de València, 2009.

[6] P. Sareh and S. D. Guest, "Design of isomorphic symmetric descendants of the miura-ori," *Smart Materials and Structures*, vol. 24, no. 8, p. 085001, 2015.

[7] T. Tachi, "Interactive freeform design of tensegrity," in *Advances in Architectural Geometry 2012*, pp. 259–268, Springer, 2013.

[8] Z. Abel, J. Cantarella, E. D. Demaine, D. Eppstein, T. C. Hull, J. S. Ku, R. J. Lang, and T. Tachi, "Rigid origami vertices: Conditions and forcing sets," *arXiv preprint arXiv:1507.01644*, 2015.

[9] T. Kawasaki, "On the relation between mountain-creases and valley-creases of a flat origami," in *Proceedings of the 1st International Meeting of Origami Science and Technology*, pp. 229–237, 1989.

[10] S. Waitukaitis and M. van Hecke, "Origami building blocks: generic and special 4-vertices," *arXiv preprint arXiv:1507.08442*, 2015.

[11] W. Gellert, *The VNR concise encyclopedia of mathematics*. Springer Science & Business Media, 2012.

[12] W. K. Schief, A. I. Bobenko, and T. Hoffmann, "On the integrability of infinitesimal and finite deformations of polyhedral surfaces," in *Discrete differential geometry*, pp. 67–93, Springer, 2008.

[13] I. Izmestiev, "Classification of flexible kokotsakis polyhedra with quadrangular base," *International Mathematics Research Notices*, p. rnw055, 2016.

[14] B. Grünbaum and G. Shephard, *Tilings and Patterns*. Series of books in the mathematical sciences, Spektrum Akademischer Verlag, 1987.

[15] H. Stachel, "Flexible polyhedral surfaces with two flat poses," *Symmetry*, vol. 7, no. 2, pp. 774–787, 2015.

[16] T. C. Hull, "Counting mountain-valley assignments for flat folds," *arXiv preprint arXiv:1410.5022*, 2014.

[17] D. E. Knuth, R. L. Graham, O. Patashnik, *et al.*, "Concrete mathematics," *Adison Wesley,*, 1989.

[18] B. Ballinger, M. Damian, D. Eppstein, R. Flatland, J. Ginepro, and T. Hull, "Minimum forcing sets for miura folding patterns," in *Proceedings of the Twenty-Sixth Annual ACM-SIAM Symposium on Discrete Algorithms*, pp. 136–147, SIAM, 2015.

[19] M. Bern and B. Hayes, "The complexity of flat origami," in *SODA*, vol. 96, pp. 175–183, 1996.